

NUMERICAL MODELING OF GEODYNAMIC PROCESSES AND LITHOSPHERE RHEOLOGY IN SUBDUCTION ZONES

Dr. Taras Gerya

Department of Geosciences, ETH-Zurich

www.erdw.ethz.ch/gerya

THEORETICAL PART

LECTURE 1:

Get started . Historical generation of concepts representing Earth's crust and mantle as visco-elasto-plastic media that can be studied with the use of partial differential equations of continuum mechanics. Fluid-like behavior of crustal and mantle rocks on geological time scale. Few words about geomodeling and geovisualisation.

Get started

In recent decades numerical modeling has become an essential approach in geosciences in general and in geodynamics in particular. This is very natural process since human direct observation scale is strongly limited in both time and space (depth) and rapid progress in computer technologies offer exceptional possibilities to explore sophisticated mathematical models of geological processes. Presently numerical modeling is inherent part of geosciences, is widely used for both testing and generating hypotheses and strongly pushing geology from observational to predictive natural science. Geomodeling and geovisualization also play strong integrating role relating different branches of geosciences. Therefore, it is almost unavoidable to have some knowledge about numerical techniques for planning and conducting state-of-the-art interdisciplinary geological research. In this respect geodynamics is traditionally strongly "infected" by numerical modeling and pushing progress of numerical methods in geosciences.

Before starting with numerical modeling we better to get read of one "myth" which is very popular among geologists often saying (or thinking) something like

"Numerical modeling is very complicated, is not affordable for persons with traditional geological background and should be done by geophysicists."

This is completely wrong but I was thinking exactly like that before I got started. I always remember my feeling when first time in my life I heard words "Navier-Stokes equation" from one of my colleagues. "Ok, forget it! This is hopeless." - thought I that time and it was wrong. Therefore, let me formulate few useful rules coming from learning experience.

Rule 1. Numerical modeling is simple and is based on simple mathematics.

All you need to know is:

- linear algebra,
- derivatives.

Most of these "complicated" mathematical knowledge we get in the school before we even start to study! I often say to my students that all is needed is non-zero MMEE index:

M: strong MOTIVATION

M: ordinary MATH

E: proper EXPLANATIONS

E: regular EXERCISES

$MMEE=M*M*E*E$ and, therefore, all four components should be non-zero. Motivation is most important, indeed...

Rule 2. When numerical modeling looks complicated see Rule 1.

Rule 3. Numerical modeling consist of solving partial differential equations (PDE).

There are only few equation to learn. They are generally not complicated but it is essential to learn and understand them gradually and properly. For example, for modeling of broad spectrum of geodynamic processes discussed in this book it is necessary to learn three principal conservation PDE:

- equation of continuity (conservation of mass),
- equation of motion (conservation of momentum - *Navier-Stokes equation!*)
- temperature equation (conservation of heat).

So, only *three* equations has to be understood and not tens or hundreds of them!

Rule 4. Read books on numerical methods several times.

There are many very good books on numerical methods. Most of these books are, however, written for physicists and engineers and need efforts to be "digested" by persons with traditional geological background (as for example that of myself).

Rule 5. Repeat transformations of equations involved into numerical modeling.

These transformations are generally standard and trivial but repeating them allows to understand structures of different PDE.

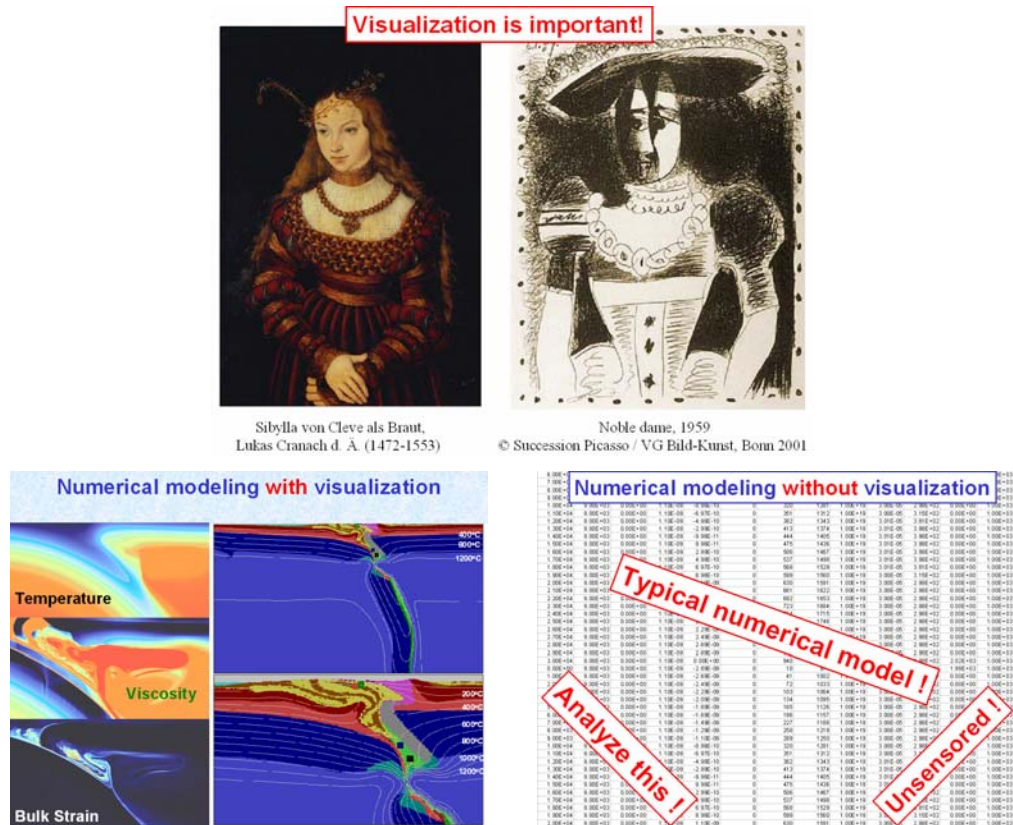


Fig. 1.1 Visualization is important!

Rule 6. Visualization is important!

Without proper visualization of results almost nothing can be done with numerical modeling (Fig. 1). Modelers often spend much more time on visualization than on computing and programming.

Rule 7. Ask!

This is the most efficient way of learning. Also, in geomodeling many small numerical know-how and "tricks" are used which are extremely important but rarely discussed in publications.

Geodynamics

Numerical modeling approaches discussed in this book are adopted for solving *thermomechanical* geodynamic problems. Geodynamics = Dynamics of the Earth is one of the core geological subjects which was very actively progressing in the last century especially since establishing of Plate Tectonics in 60th. Broad introducing of thermodynamics to mineralogy and petrology was about that time as well. This was really great time for geology which "drifted" strongly from descriptive qualitative to predictive quantitative physical science. The overall history of development of Geodynamics was not, indeed, very "dynamic" but rather slow and complicated. Excellent introduction to this field by Donald L. Turcotte and Gerald Schubert (1982, 2002) discuss the following important historical steps of understanding of the Earth as dynamic system

1620: *Francis Bacon, Pointing out of similarity in shape between the west coast of Africa and the east coast of South America.*

This was about 400 (!) years ago and several centuries needed to start interpreting this similarity.

Later part of 19th century: *establishing of fluid like behavior of the Earths' mantle based on gravity studies: mounting ranges have low-density roots.*

This crucial finding was only "coupled" to Earth dynamics one hundred year later and was not explored in the continental drift hypothesis.

1910: *Frank B. Taylor, Continental Drift hypothesis.*

Real beginning of "drifting" toward plate tectonics, still long way to go.

1912-1946: *Alfred Wegener, further developed Continental Drift hypothesis, showed correspondence of geological provinces, relict mountain ranges and fossil types. Driving forces - tidal / rotation of the Earth. Single protocontinent - Pangea.*

The principal question is considered to be "Why the continents move? What are driving forces" and not yet "How the continents move? What is movement mechanism?"

1924: *Harold Jeffreys, showed insufficiency of Wegener's forces to move continents.*

Computing forces for testing geodynamic hypothesis. This is one of the core principles of modern geodynamics as well! Another point to learn – opposing of continental drift hypothesis using physical arguments was always strong and probably strongly delayed creating of plate tectonics.

1931: *Arthur Holmes, suggested that thermal convection in the Earth's mantle can drive continental drift.*

This crucial idea answered question about driving forces but not about movement mechanisms. It was known after seismic studies that Earth's mantle is in solid state and been deformed elastically must not allow thousand kilometers "travelling" of the continents.

1935: *N.A.Haskell, establishing of fluid-like behavior of mantle (viscosity 10^{20} Pa s) based on the analyses of beach terraces in Scandinavia. Post-glaciation rebound.*

Actually this was also established much early from observing of crustal roots. The question about physical mechanisms of solid-state mantle deformations remains open.

1937: *Alexander du Toit, suggested existence of two protocontinents - Laurasia and Gondwanaland - separated by Tethys ocean.*

This is really dramatic story: geologists were continuously developing continental drift hypothesis but general idea of large lateral displacements of the continents was continuously rejected by geophysicists.

1950s: *finding of mid-ocean ridges*

Evidence are critically growing...

1950s: *findings of mechanisms of solid state creep of crystalline materials, applicable for example for the flow of ice in glaciers.*

The answer to the second crucial question was finally found in material science!

Great 60th have started!

1960s: *Paleomagnetic studies, finding of regular patterns of magnetic anomalies on the sea floor.*

1962: *Harry Hess, Seafloor Spreading hypothesis.*

1965: *B.Gordon, quantitative link between solid state creep and mantle viscosity.*

1968: *Jason Morgan, Basic hypothesis of Plate Tectonic (mosaic of rigid plates in relative motion with respect to one another as a natural consequence of mantle convection).*

1968: *Isacks et al., attributing of earthquakes, volcanoes, and mountain building to plate boundaries.*

1967-1970: *Development and broad accepting of Plate Tectonics.*

Before this time continental drift was strongly opposed by geophysicists based on rigidity of solid mantle and "absence" of mechanism providing horizontal displacements of thousands of kilometers for continents.

Crucial point that was finally understood by geological community is that both viscous (i.e., fluid-like) and elastic (i.e., solid-like) behavior is characteristic for the Earth depending on the time scale: Earth's mantle which is elastic on human time scale is indeed viscous on geological time scale (>10,000 years) and can be strongly internally deformed due to the solid state creep. There is an amazing substance demonstrating similar "dual" viscous-elastic behavior. This is silicon putty or "silly putty" used as analog of rocks in experimental tectonics. It deforms like a clay in hands but when dropped on the floor jumps up like a rubber ball.

Plate tectonics has largely established both conceptual and physical basis of Geodynamics. Further rapid spreading of numerical methods of mechanics of continuum in this field is a logical consequence of both theoretical and technological progress. Numerical modeling is an inherent tool for geodynamics since tectonic processes are often too slow to observe them directly.

Few words about geomodeling and geovisualisation

At present geomodeling and geovisualization are extremely actively developing fields. In the field of geodynamics many modeling and visualization challenges still exist for example

geodynamic modeling challenges

- a) Realistic physical properties of rocks
- b) Phase transformations, melting
- c) Fluid and melt transport in deforming systems

- d) Geochemical processes
- e) Ultrahigh resolution (multiple-scales grids, adaptive grids)
- f) 3D

geodynamic visualization challenges

- a) Geology-friendliness
- b) Ultrahigh resolution
- c) Multiple-scales
- d) Multiple-aspects
- e) 3D

In frame of this guide MatLab is used for exercises in numerical modeling and visualization. This is good language of choice for the beginners which allows both easy computing and visualization. C and FORTRAN are often used for advanced numerical studies involving the use of supercomputers. In this studies visualization is mostly done as post-processing of computed data which allows to use specialized 2D and 3D visualization packages. In our short course we are more interested to see results instantaneously during computing. In addition MatLab greatly simplify solving of system of linear equations which is the core of numerical modeling.

Basic books:

- I. *Donald L. Turcotte and Gerald Schubert, Geodynamics. Second edition. Cambridge University Press, 2002*
- II. *Giorgio Ranalli Rheology of the Earth. Kluwer Academic Publishers, 1995*
- III. *Leon Lapidus, George F. Pinder, Numerical Solution of Partial Differential Equations in Science and Engineering. John Wiley & Sons, 1999.*

LECTURE 3:

Definition of geological media as a continuum. Vector and scalar field variables used for representation of continuum. Methods of continuous and discrete definition of field variables. Continuity equation. Continuity equation for incompressible fluid and its application for geodynamic problems.

An important understanding that we need before starting with differential equations is that in geodynamics we are dealing with *continuous geological medium* (Earth's crust and mantle). *Continuity* of this medium implies that on a macroscopic scale it does not contain voids and gaps and consists of intercalating different rocks and, some times, melts. Various physical properties of continuum may be different in every geometrical point and, thus, need *continuous description*. In the *mechanics of continuum* physical (field) properties of a continuum are described by *field variables* (P, T, density, velocity etc.). There are three major types of field variables:

scalars (e.g., P, T, density),

vectors (e.g., velocity, heat flux) and

tensors (e.g. stress, strain rate).

Field variables can be represented by *fully continuous* way (analytical expressions) and by *discrete-continuous* way (by arrays of values characterizing selected *nodal* geometrical points). In the later case various linear and non-linear *interpolation* rules are used to calculate values of field variables between the nodal points.

Continuity also implies that displacements of different portions of the medium are not fully independent. These displacement must proceed in such a way that will not create macroscopic voids and gaps: if some rocks are displaced *from* certain area (for example due to tectonic extrusion), other rocks must come *into* this area and substitute displaced fragment. In a way this type of continuous behavior is very similar to the behavior of water or, generally, any fluid. Therefore geodynamics processes in the Earth's mantle, as for example mantle convection, are often referred to as processes of *geophysical fluid dynamics*. Our intuitive qualitative understanding of continuity can, indeed, be transformed to the nice quantitative mathematical formalisms. This formalism is widely used in numerical geodynamic modeling in form of *continuity equation* describing *conservation of mass* during displacement of continuous medium

Eulerian continuity equation (i.e., written for immobile *Eulerian observation point*) has a form

$$\partial\rho/\partial t + \text{div}(\rho\underline{v}) = 0, \quad (3.1)$$

Lagrangian continuity equation (i.e., written for moving *Lagrangian material point*) has a form

$$D\rho/Dt + \rho\text{div}(\underline{v}) = 0, \quad (3.2)$$

where ρ is density (*scalar*) characterizing amount of mass per unit volume in either Eulerian or Lagrangian point, \underline{v} - velocity (vector) in this point.

Understanding differences between Eulerian (observation) and Lagrangian (material) geometrical points is fundamental for mechanics of continuum. Lagrangian point is strictly connected to the material point and is moving with this point. Therefore, the same material point is always found in a given Lagrangian point independent of the moment of time. For this reason Lagrangian time derivative of density $D\rho/Dt$ (i.e., changes of density with time in the Lagrangian point) is also called *substantive* or *objective* time derivative. On the other hand, Eulerian point is an immobile observation point which is not related to specific material point. Therefore, in different moments of time different material points can be found in given Eulerian point. Another word, different material points are *passing through* the Eulerian observation point with time. Many equations of mechanics of continuum

containing time derivatives can be written in both Eulerian and Lagrangian form that differ from each other, for example Eqs. (3.1) and (3.2).

Let's now analyze the continuity equation which contains both vector (velocity) and scalar (density) variables. In every geometrical point velocity vector can be defined by its three components $\underline{v} = (v_x, v_y, v_z)$, corresponding to three principal axis x, y and z

Continuity equation looks pretty short and simple but, as it is often happen with PDE, both the simplicity and the shortness are apparent. Continuity equation establish balance of mass in an elementary volume. It implies, in particular, that if mass is leaving (fluxing out of) the volume (i.e., $\text{div}(\rho\underline{v}) > 0$), local density (i.e., the amount of mass per unit volume) decreases with time (i.e., $\partial\rho/\partial t < 0$).

The following derivations "decipher" contents of continuity equation

$\rho\underline{v}$ is the vector of *mass flux* through a geometrical point $\rho\underline{v} = (\rho v_x, \rho v_y, \rho v_z)$

$\text{div}(\rho\underline{v})$ is a *divergence* of mass fluxes characterizing overall balance of incoming and outgoing fluxes in the geometrical point. It is convenient to decompose $\text{div}(\rho\underline{v})$ according to the standard differentiation rules

$$\text{div}(\rho\underline{v}) = \rho \text{div}(\underline{v}) + \underline{v} \text{grad}(\rho) \quad (3.3)$$

where $\text{div}(\underline{v})$ is divergence of velocity vector \underline{v} . Divergence of a vector is a scalar

$$\text{div}(\underline{v}) = \partial v_x / \partial x + \partial v_y / \partial y + \partial v_z / \partial z \quad (3.4)$$

and therefore

$$\rho \text{div}(\underline{v}) = \rho \partial v_x / \partial x + \rho \partial v_y / \partial y + \rho \partial v_z / \partial z \quad (3.5)$$

On the other hand, $\text{grad}(\rho)$ is gradient of density ρ . Gradient of scalar is a vector

$$\underline{\text{grad}}(\rho) = (\partial\rho/\partial x, \partial\rho/\partial y, \partial\rho/\partial z) \quad (3.6)$$

and therefore

$$\underline{v} \text{grad}(\rho) = v_x \partial\rho/\partial x + v_y \partial\rho/\partial y + v_z \partial\rho/\partial z \quad (3.7)$$

$\underline{v} \text{grad}(\rho)$ is *advective transport* term that reflect changes of density in the immobile (Eulerian) point due to the movement of inhomogeneous medium with existing density gradients relatively to this point. In case when density in all moving material points remains constant Eulerian continuity equation reduces to the *advective transport equation*

$$\partial\rho/\partial t + \underline{v} \text{grad}(\rho) = 0 \quad (3.9)$$

or

$$\partial\rho/\partial t = -v_x \partial\rho/\partial x - v_y \partial\rho/\partial y - v_z \partial\rho/\partial z \quad (3.10)$$

Minus in the right part of equation (3.10) reflects obvious relation between density gradient and direction of motion: if medium is moving *in the direction* of increasing density (i.e. $v_x \partial\rho/\partial x > 0$ in 1-D case) then density in the immobile observation point *decreases* with time (i.e., $\partial\rho/\partial t < 0$). We will come back again to advective transport equation in the Lecture 10.

On the other hand *substantive* changes of density ($D\rho/Dt$) in the moving Lagrangian point does not depend on density gradients and Lagrangian continuity equation (3.2) does not contain advective terms.

For geological medium incompressibility condition ($\rho = \text{const}$, $D\rho/Dt = 0$ or $\partial\rho/\partial t + \underline{v} \text{grad}(\rho) = 0$) is often valid so that one can write *incompressible continuity equation* in the incompressible form which is the same for both Eulerian and Lagrangian points

$$\text{div}(\underline{v}) = 0 \quad (3.11)$$

Solve the following example:

In some region of the Earth's mantle velocity field is given by equation

$$v_x = 10^{-10} + x10^{-13} + y10^{-13} + z10^{-13}$$

$$v_y = 10^{-10} - x10^{-13} + 2y10^{-13} + 3z10^{-13}$$

$$v_z = 10^{-10} - x10^{-13} - y10^{-13} - 2z10^{-13}$$

density field is given by

$$\rho = 3300 + 0.001x - 0.002y + 0.001z$$

Please calculate: ρ , $\text{div}(\underline{v})$, $\partial\rho/\partial t$ and $D\rho/Dt$ for the point with coordinates $x=1000$, $y=1000$, $z=1000$,

Application for geodynamic problems - corner flow at subduction zones - continuity driven circulation in subduction channels.

LECTURE 4.

Deformation and stresses. Definition of stress and strain-rate tensors. Deviatoric stresses. Mean stress as a dynamic (non-lithostatic) pressure. Orientation of stress axes. Transformations of tensors. Tensor invariants.

Tensors are field variables which characterize internal state of continuum and are, perhaps, most difficult for intuitive understanding. Indeed, at least two of them we have to use in the following and these are *stress* and *strain rate* tensors.

Stresses are forces per unit area that are transmitted through a material by interatomic force field. *Normal stresses* are transmitted perpendicular to a surface. *Shear stresses* are transmitted parallel to a surface. In three dimensions we have 9 components of stress denoted as σ_{ij} , where i and j are coordinates (x, y, z or 1, 2, 3 as often used in the mechanics of continuum) so that

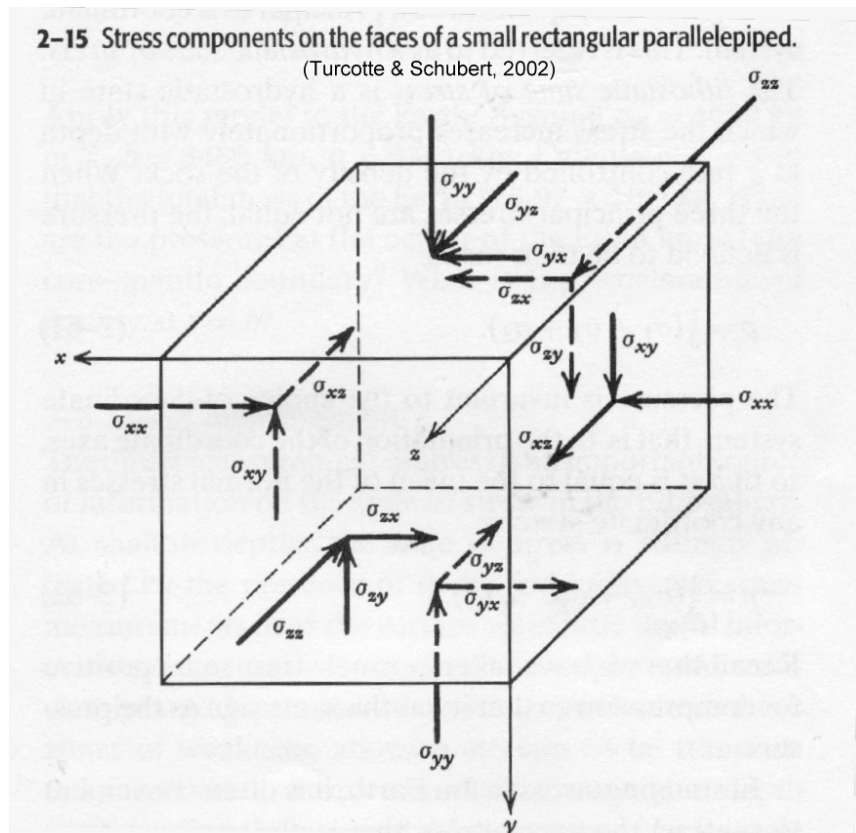
three normal stresses:

$$\sigma_{xx}, \sigma_{yy}, \sigma_{zz},$$

six shear stresses corresponding to the *condition of force balance* $\sigma_{ij} = \sigma_{ji}$:

$$\sigma_{xy} = \sigma_{yx}, \quad \sigma_{xz} = \sigma_{zx}, \quad \sigma_{yz} = \sigma_{zy},$$

First index (i) denote the axes which is perpendicular to the considered surface and the second index (j) denote the axes parallel to the force component.



Here and further we will take normal extensional stresses as positive and compressional as negative. This is most common convention (but not the only convention) for mechanics of continuum. Similarly to components of vectors stress components change with changing coordinate system.

In continuum mechanics *pressure* is defined as mean normal stress

$$P = -(\sigma_{xx} + \sigma_{yy} + \sigma_{zz})/3 \tag{4.1}$$

Minus in the right part of Eq. (4.1) reflect another convention according to which pressure is positive under compression. Pressure is stress *invariant* and, thus, *does not change with changing the coordinate system*. In case of hydrostatic stress state all shear stresses are zero and all normal stresses are equal to each other

$$\begin{aligned}\sigma_{xy}=\sigma_{yx}=\sigma_{xz}=\sigma_{zx}=\sigma_{yz}=\sigma_{zy}=0 \\ \sigma_{xx} = \sigma_{yy} = \sigma_{zz} = -P\end{aligned}$$

In geosciences pressure is often considered as corresponding to these hydrostatic (*lithostatic*) conditions and is computed as a function of depth and vertical density profile

$$\rho_{\text{rock}} = g \sum_{i=1}^n \rho_i X_i . \quad (4.2)$$

This simplification does not hold when deformations of geological media occur and real *dynamic* pressure may notably deviate from the lithostatic value given by Eq. (4.2).

It is convenient to define *deviatoric* stresses (σ'_{ij}), which are deviations of stresses from hydrostatic stress state

$$\sigma'_{ij} = \sigma_{ij} + P \delta_{ij}, \quad (4.3)$$

where δ_{ij} is the Kronecker delta: $\delta_{ij}=1$ when $i=j$ and $\delta_{ij}=0$ when $i \neq j$, i and j are coordinates (x, y, z). Kronecker delta is quite peculiar abbreviation commonly used in the mechanics of continuum. It only takes values of either 1 or 0 and is in fact analogous to the logical operator "if" used in many programming languages. Any equation with δ_{ij} represent *group of equations*. For example Eq. (4.2) in 3-D represent the following equations

normal deviatoric stresses

$$\begin{aligned}\sigma'_{xx} &= \sigma_{xx} + P \\ \sigma'_{yy} &= \sigma_{yy} + P \\ \sigma'_{zz} &= \sigma_{zz} + P\end{aligned}$$

shear stresses which are all deviatoric

$$\begin{aligned}\sigma'_{xy} &= \sigma_{yx} = \sigma_{xy} = \sigma_{yx}, \\ \sigma'_{xz} &= \sigma_{zx} = \sigma_{xz} = \sigma_{zx}, \\ \sigma'_{yz} &= \sigma_{zy} = \sigma_{yz} = \sigma_{zy}.\end{aligned}$$

It worth mentioning that the sum of normal deviatoric stresses is zero by definition (Eq. 4.1)

$$\sigma'_{xx} + \sigma'_{yy} + \sigma'_{zz} = 0$$

since

$$\sigma_{xx} + \sigma_{yy} + \sigma_{zz} = -3P$$

Second invariant of deviatoric stress tensor can be calculated as follows

$$(\sigma_{II})^2 = 1/2(\sigma'_{ij})^2 \quad (4.4)$$

Index ij in equation (4.4) denote *summation*! This is another abbreviation that is commonly used in continuum mechanics and which makes equations shorter (but, indeed, not easier to understand for beginners). Complete "deciphered" form of Eq. (4.4) looks much longer

$$(\sigma_{II})^2 = 1/2[(\sigma'_{xx})^2 + (\sigma'_{yy})^2 + (\sigma'_{zz})^2 + (\sigma'_{xy})^2 + (\sigma'_{yx})^2 + (\sigma'_{xz})^2 + (\sigma'_{zx})^2 + (\sigma'_{yz})^2 + (\sigma'_{zy})^2], \quad (4.5)$$

or, using condition of force balance $\sigma_{ij} = \sigma_{ji}$

$$(\sigma_{II})^2 = 1/2[(\sigma'_{xx})^2 + (\sigma'_{yy})^2 + (\sigma'_{zz})^2 + \sigma_{xy}^2 + \sigma_{xz}^2 + \sigma_{yz}^2]. \quad (4.6)$$

Second stress invariant σ_{II} does not depend on the coordinate system and characterizes quantitative degree of deviation of the system from the hydrostatic (lithostatic) state.

Another very important tensor which we will use in the following is *strain rate* $\dot{\epsilon}_{ij}$ that characterizes *rate* of internal deformation of continuum. In fact, $\dot{\epsilon}_{ij}$ is time derivative of *strain* tensor ϵ that characterizes internal deformation itself. Strain is dimensionless and is computed as the ratio of absolute value of deformation to the length of deforming body. By analogy with stress one can discriminate normal and shear components of strain corresponding to axial and shear deformation, respectively.

Indeed in numerical geodynamic modeling it is often convenient to use *strain rates* characterizing dynamics of changes in the internal deformation rather than strain characterizing absolute value of this deformation. Components of strain rate tensor are defined via spatial gradients of velocity as follows

$$\dot{\epsilon}_{ij} = \frac{1}{2} \left(\frac{\partial v_i}{\partial j} + \frac{\partial v_j}{\partial i} \right)$$

where i and j are coordinates (x, y, z) so that

normal strain rate components

$$\dot{\epsilon}_{xx} = \frac{1}{2} \left(\frac{\partial v_x}{\partial x} + \frac{\partial v_x}{\partial x} \right) = \frac{\partial v_x}{\partial x}$$

$$\dot{\epsilon}_{yy} = \frac{1}{2} \left(\frac{\partial v_y}{\partial y} + \frac{\partial v_y}{\partial y} \right) = \frac{\partial v_y}{\partial y}$$

$$\dot{\epsilon}_{zz} = \frac{1}{2} \left(\frac{\partial v_z}{\partial z} + \frac{\partial v_z}{\partial z} \right) = \frac{\partial v_z}{\partial z}$$

shear strain rate components

$$\dot{\epsilon}_{xy} = \dot{\epsilon}_{yx} = \frac{1}{2} \left(\frac{\partial v_x}{\partial y} + \frac{\partial v_y}{\partial x} \right)$$

$$\dot{\epsilon}_{xz} = \dot{\epsilon}_{zx} = \frac{1}{2} \left(\frac{\partial v_x}{\partial z} + \frac{\partial v_z}{\partial x} \right)$$

$$\dot{\epsilon}_{yz} = \dot{\epsilon}_{zy} = \frac{1}{2} \left(\frac{\partial v_y}{\partial z} + \frac{\partial v_z}{\partial y} \right)$$

Symmetric form of strain rate tensor subtract rotational component of velocity field which does not contribute to the deformation: it is easy to check that rotation of rigid body in 2-D has gradients in

velocity field but does not produce any internal deformation, i.e. $\dot{\epsilon}_{ij} = \frac{1}{2} \left(\frac{\partial v_i}{\partial j} + \frac{\partial v_j}{\partial i} \right) = 0$

Second invariant of strain rate tensor is calculated as follows

$$\dot{\epsilon}_{II}^2 = \frac{1}{2} \dot{\epsilon}_{ij}^2 \text{ (by analogy of } \sigma_{II}^2 \text{ formula given above)}$$

By analogy to stress tensor strain rate can also be subdivided to isotropic and deviatoric components. *Deviatoric* strain rates ($\dot{\epsilon}_{ij}'$) are formulated as follows

$$\dot{\epsilon}_{ij}' = \dot{\epsilon}_{ij} - \delta_{ij} \frac{1}{3} \dot{\epsilon}_{kk}$$

$$\dot{\epsilon}_{kk} = \dot{\epsilon}_{xx} + \dot{\epsilon}_{yy} + \dot{\epsilon}_{zz} = \text{div}(\bar{v})$$

Accordingly $\dot{\epsilon}_{xx}' + \dot{\epsilon}_{yy}' + \dot{\epsilon}_{zz}' = 0$

Reading: Turcotte & Schubert, 2002, p. 80-87, Ranalli, 1995, Chapters 2.6-2.8.

LECTURE 5.

Viscosity and Newtonian law of viscous friction. Navie-Stokes equation of motion for viscous fluid. Stokes equation of slow laminar flow for highly viscous incompressible fluid and its application for geodynamics.

As we discussed in our first lecture on geological time scale rocks often behave as highly viscous fluid. For this reason viscous *rheological* relationship between stress and strain rate known as *Newtonian law of viscous friction* is broadly used in geodynamic modeling. Newtonian law of viscous friction relate shear stress τ (Pa) with shear strain rate $\frac{\partial v}{\partial x}$ (1/s)

$$\tau = \eta \frac{\partial v}{\partial x} \quad (5.1)$$

where η (Pa s) is the viscosity which characterizes degree of resistance of material to shear deformation. Generally viscosity is different for different materials and may also depend on pressure (P), temperature (T), strain rate and some other parameters. Typically viscosity of rocks is greater than 10^{17} Pa s: viscosity of asthenospheric upper mantle, for example, is on the order of 10^{21} Pa s. We will discuss this issue in more details in the next lecture.

In case of 3-D deformation of a fluid the law of viscous friction is formulated via components of deviatoric stress (σ_{ij}') and strain rate ($\dot{\epsilon}_{ij}'$) tensors as follows

$$\sigma_{ij}' = 2\eta \dot{\epsilon}_{ij}' + \delta_{ij}\eta_b \dot{\epsilon}_{kk} = 2\eta(\dot{\epsilon}_{ij} - 1/3 \delta_{ij}\dot{\epsilon}_{kk}) + \delta_{ij}\eta_{\text{bulk}} \dot{\epsilon}_{kk}$$

where where i and j are coordinates (x, y, z); η and η_{bulk} are shear and bulk viscosity, respectively; δ_{ij} is the Kronecker delta: $\delta_{ij}=1$ when $i=j$ and $\delta_{ij}=0$ when $i \neq j$; ϵ_{kk} is the sum of normal components of strain rate tensor reflecting *inelastic* volume changes (i.e., due to phase transformations):

$$\dot{\epsilon}_{kk} = \dot{\epsilon}_{xx} + \dot{\epsilon}_{yy} + \dot{\epsilon}_{zz} = \text{div}(\underline{v})$$

In the absence of mineralogical phase transformations rocks are characterized by insignificant density variations. Therefore *incompressible fluid approximation* ($\rho=\text{const}$, $D\rho/Dt=0$, see Lecture 3) is often valid. In this case $\text{div}(\underline{v})=0$, $\dot{\epsilon}_{kk}=0$, $\dot{\epsilon}_{ij}' = \dot{\epsilon}_{ij}$ and the law of viscous friction is simplified as follows

$$\sigma_{ij}' = 2\eta \dot{\epsilon}_{ij}' .$$

Deformation of viscous fluid is always result of internal and external forces acting on this fluid. In order to relate forces and deformation an equation of force balance should be used. This is so *called Navie-Stokes equation of motion* which describe *conservation of momentum* for viscous fluid in the gravity field

$$\frac{\partial \sigma_{ij}'}{\partial j} - \frac{\partial P}{\partial i} + \rho g_i = \rho \frac{Dv_i}{Dt} \quad (5.2)$$

where i and j are coordinates (x, y, z); g_i is i -th component of gravity vector \bar{g} ; $\frac{Dv_i}{Dt}$ is substantive time derivative of i -th component of velocity vector (i.e., acceleration). By analogy to other substantive time derivatives

$$\frac{Dv_i}{Dt} = \frac{\partial v_i}{\partial t} + \bar{v} \text{grad}(v_i)$$

for example

$$\frac{Dv_x}{Dt} = \frac{\partial v_x}{\partial t} + v_x \frac{\partial v_x}{\partial x} + v_y \frac{\partial v_x}{\partial y} + v_z \frac{\partial v_x}{\partial z}$$

In case of 3-D deformation Navie-Stokes equation of motion corresponds in fact to the system of three different equations

$$x\text{-Navie-Stokes equation } \frac{\partial \sigma_{xx}'}{\partial x} + \frac{\partial \sigma_{xy}'}{\partial y} + \frac{\partial \sigma_{xz}'}{\partial z} - \frac{\partial P}{\partial x} + \rho g_x = \rho \frac{Dv_x}{Dt}$$

$$y\text{-Navie-Stokes equation } \frac{\partial \sigma_{yy}'}{\partial y} + \frac{\partial \sigma_{yx}'}{\partial x} + \frac{\partial \sigma_{yz}'}{\partial z} - \frac{\partial P}{\partial y} + \rho g_y = \rho \frac{Dv_y}{Dt}$$

$$z\text{-Navie-Stokes equation } \frac{\partial \sigma_{zz}'}{\partial z} + \frac{\partial \sigma_{zx}'}{\partial x} + \frac{\partial \sigma_{zy}'}{\partial y} - \frac{\partial P}{\partial z} + \rho g_z = \rho \frac{Dv_z}{Dt}$$

In case of highly viscous flows inertial forces ($\rho \frac{Dv_i}{Dt}$) are negligible by comparison to viscous resistance and gravity forces and deformation of fluid can be accurately described by the *Stokes equation of slow flow*

$$\frac{\partial \sigma_{ij}'}{\partial j} - \frac{\partial P}{\partial i} + \rho g_i = 0, \quad (5.3)$$

or

$$x\text{-Stokes equation } \frac{\partial \sigma_{xx}'}{\partial x} + \frac{\partial \sigma_{xy}'}{\partial y} + \frac{\partial \sigma_{xz}'}{\partial z} - \frac{\partial P}{\partial x} + \rho g_x = 0$$

$$y\text{-Stokes equation } \frac{\partial \sigma_{yy}'}{\partial y} + \frac{\partial \sigma_{yx}'}{\partial x} + \frac{\partial \sigma_{yz}'}{\partial z} - \frac{\partial P}{\partial y} + \rho g_y = 0$$

$$z\text{-Stokes equation } \frac{\partial \sigma_{zz}'}{\partial z} + \frac{\partial \sigma_{zx}'}{\partial x} + \frac{\partial \sigma_{zy}'}{\partial y} - \frac{\partial P}{\partial z} + \rho g_z = 0$$

Even more simplifications can be done for the homogeneous incompressible fluid with very high constant viscosity. In this case the Stokes equation is simplified to

$$\eta \frac{\partial^2 v_i}{\partial j^2} - \frac{\partial P}{\partial i} + \rho g_i = 0 \quad (5.4)$$

In case of 3D deformation we as usually have three equations

$$\eta \left(\frac{\partial^2 v_x}{\partial x^2} + \frac{\partial^2 v_x}{\partial y^2} + \frac{\partial^2 v_x}{\partial z^2} \right) - \frac{\partial P}{\partial x} + \rho g_x = 0 \quad \text{or} \quad \eta \Delta v_x = \frac{\partial P}{\partial x} - \rho g_x$$

$$\eta \left(\frac{\partial^2 v_y}{\partial x^2} + \frac{\partial^2 v_y}{\partial y^2} + \frac{\partial^2 v_y}{\partial z^2} \right) - \frac{\partial P}{\partial y} + \rho g_y = 0 \quad \text{or} \quad \eta \Delta v_y = \frac{\partial P}{\partial y} - \rho g_y$$

$$\eta \left(\frac{\partial^2 v_z}{\partial x^2} + \frac{\partial^2 v_z}{\partial y^2} + \frac{\partial^2 v_z}{\partial z^2} \right) - \frac{\partial P}{\partial z} + \rho g_z = 0 \quad \text{or} \quad \eta \Delta v_z = \frac{\partial P}{\partial z} - \rho g_z$$

where $\Delta = \frac{\partial^2}{\partial x^2} + \frac{\partial^2}{\partial y^2} + \frac{\partial^2}{\partial z^2}$ is *Laplace operator*.

When pressure gradient is constant ($\eta \frac{\partial^2 v_i}{\partial j^2} - \frac{\partial P}{\partial i} + \rho g_i = 0$) Stokes equation can be written in form of *Poisson equation*

$$\Delta v_i = \text{const} \quad (5.5)$$

where

$$\text{const} = \frac{1}{\eta} \left(\frac{\partial P}{\partial i} - \rho g_i \right)$$

In 3-D this is (as usually) the system of three equations which are always good to write explicitly

$$x\text{-Poisson equation } \Delta v_i = \text{const}, \text{ where } \text{const} = \frac{1}{\eta} \left(\frac{\partial P}{\partial i} - \rho g_i \right)$$

$$y\text{-Poisson equation } \Delta v_i = \text{const}, \text{ where } \text{const} = \frac{1}{\eta} \left(\frac{\partial P}{\partial i} - \rho g_i \right)$$

$$z\text{-Poisson equation } \Delta v_i = \text{const}, \text{ where } \text{const} = \frac{1}{\eta} \left(\frac{\partial P}{\partial i} - \rho g_i \right)$$

Dispite the simplicity Poisson equation is valid for several important geodynamic problems, for example for the uniaxial (e.g. purely vertical) flow of a fluid in a channel (e.g. magma flow in the magmatic channel, rock flow in the subduction channel etc.)

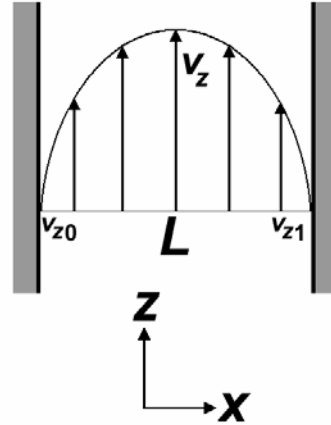


Figure. 5.1. Planar flow of viscous fluid in the channel.

In case of planar channel $v_x=0$, $v_y=0$, $\frac{\partial v_z}{\partial z} = 0$, $\frac{\partial v_z}{\partial y} = 0$ and the system of three Poisson equations reduces to

$$\frac{\partial^2 v_z}{\partial x^2} = \frac{1}{\eta} \left(\frac{\partial P}{\partial z} - \rho g_z \right) \quad (5.6)$$

which can be solved analytically by two-fold integration as

$$v_z(x) = \frac{1}{2\eta} \left(\frac{\partial P}{\partial z} - \rho g_z \right) x^2 + C_1 x + C_2$$

where C_1 and C_2 are integration constants which can be defined from the boundary conditions

$$v_z(x) = v_{z0} \text{ when } x = 0$$

and

$$v_z(x) = v_{z1} \text{ when } x = L \text{ (} L \text{ is the channel width)}$$

then $C_2 = v_{z0}$ and $C_1 = \frac{v_{z1} - v_{z0}}{L} - \frac{1}{2\eta} \left(\frac{\partial P}{\partial z} - \rho g_z \right) L$.

Analytical exercises with the Poisson equation are, indeed, very useful as analytical solutions are often used for *benchmarking* (i.e., testing accuracy) numerical solutions.

Exercise. Please calculate vertical velocity of magma flow (v_z) in the middle of the planar channel of width $L = 100$ m, if viscosity of magma is $\eta = 10^{16}$ Pa s and its density is $\rho = 2800$ kg/m³.

Pressure gradient along the channel is $\frac{\partial P}{\partial z} = -25000$ Pa/m. Acceleration of gravity is $g_z = -10$ m/s² (i.e. gravity acceleration is directed downward). Velocity on the channel boundaries is zero. Please derive the solution for the case when right boundary is moving upward with velocity $v_{z1} = 10^{-3}$ m/s

Reading: Turcotte & Schubert, 2002, p. 226-237, Ranalli (1995), chapters 4.1-4.3.

Turcotte & Schubert, 2002, p. 80-87, Ranalli, 1995, Chapters 2.6-2.8.

LECTURE 6.

Rheological equations. Effective viscosity and its dependence on temperature, pressure, and deformation rate.

Now let's discuss in more details viscosity and, generally, rheology of rocks reflecting peculiarities of solid-state creep, which is the major mechanism of rock deformation. Solid-state creep is an ability of crystalline substances to deform irreversibly under applied stresses. Solid-state creep is the major deformation mechanism of the Earth's crust and mantle. Two major type of the creep are known: *diffusion creep* and *dislocation creep*.

Diffusion creep is typically observed at relatively low stresses and results from the diffusion of atoms through the interior (Herring-Nabarro creep) and along the boundaries (Coble creep) of crystalline grains subjected to stresses. As the result of this diffusion, the grains deform which also lead to the bulk rock deformation.

Diffusion creep is characterized by linear relationship between strain rate and stress (i.e., Newtonian law $\tau = \eta \frac{\partial v}{\partial x}$) with viscosity (η) independent of strain rate and dependent on pressure (P), temperature (T) and grain size (h)

$$\eta = \frac{RTh^2}{24V_a D_0} \exp\left(\frac{E_a + V_a P}{RT}\right) \text{ for Herring-Nabarro creep} \quad (6.1)$$

$$\eta = \frac{RTh^3}{24V_a b D_{b0}} \exp\left(\frac{E_a + V_a P}{RT}\right) \text{ for Coble creep}$$

where R is the gas constant, D_0 and D_{b0} are, respectively, intergranular and boundary diffusion constants; b is the width of grain boundary; E_a and V_a are, respectively, activation energy and activation volume. Typical values of activation energy vary from 100 to 600 kJ/mol depending on rock/mineral composition, presence of fluid, oxygen fugacity etc.

Dislocation creep is observed at higher stresses and results from migration of dislocations (imperfections in the crystalline lattice structure). Dislocation density strongly depends on stresses, and therefore dislocation creep results in non-linear (*non-Newtonian*) relationship between strain rate and stress

$$\dot{\epsilon} = A(\sigma')^n \quad (6.2)$$

where A is material constant and $n > 1$ (typically $n=3$). In case of dislocation creep an *effective viscosity* dependent on stress can be used to characterize non-Newtonian rheology

$$\eta_{eff} = \frac{\sigma'}{2\dot{\epsilon}} \quad (6.3)$$

When $n=3$ effective viscosity for dislocation creep can be calculated as follows

$$\eta_{eff} = \frac{RT(BG)^2}{24V_a D_0} \frac{1}{(\sigma')^2} \exp\left(\frac{E_a + V_a P}{RT}\right) \quad (6.4)$$

where B is magnitude of the Burgers vector for the dislocation and G is shear modulus.

Both dislocation and diffusion creep can occur simultaneously leading to the following relation for the effective viscosity

$$1/\eta_{eff} = 1/\eta_{dist} + 1/\eta_{diff} \quad (6.5)$$

This relation follows from the assumption that under condition of constant applied deviatoric stress σ' strain rate $\dot{\epsilon}_{ij}$ can be decomposed to the contribution of dislocation ($\dot{\epsilon}_{ij}^{\text{disl}}$) and diffusion ($\dot{\epsilon}_{ij}^{\text{diff}}$) creep, each of these contributions correspond to relation (6.3)

$$\dot{\epsilon}_{ij} = \dot{\epsilon}_{ij}^{\text{disl}} + \dot{\epsilon}_{ij}^{\text{diff}} \quad (6.6)$$

where

$$\dot{\epsilon}_{ij} = \sigma' / (2\eta_{\text{eff}}), \quad \dot{\epsilon}_{ij}^{\text{disl}} = \sigma' / (2\eta_{\text{disl}}), \quad \dot{\epsilon}_{ij}^{\text{diff}} = \sigma' / (2\eta_{\text{diff}}) \quad (6.7)$$

Please, substitute relations (6.7) to equation (6.6) and get formula (6.5).

Both diffusion and dislocation creep rheology are often calibrated from experimental data using simple parameterized relationship between applied differential stress $\sigma_d = 2(\sigma_{\text{II}}^2)^{1/2}$ (i.e. difference between maximal and minimal applied stress) and resulted ordinary strain rate $\dot{\gamma}_{ij} = \frac{\partial v_i}{\partial j}$ (not a component of the strain rate tensor $\dot{\epsilon}_{ij}$)

$$\dot{\gamma} = A_D (\sigma_d)^n \exp\left(-\frac{E_a + V_a P}{RT}\right) \quad (6.8)$$

where A_D , n , E_a and V_a are experimentally determined rheological parameters. In order to use such experimentally parameterized relation in numerical modeling one need to reformulate it in term of stress and strain rate invariants corresponding to the relation (6.3), i.e.

$$\eta_{\text{eff}} = \sigma_{\text{II}} / (2\dot{\epsilon}_{\text{II}})$$

For this purpose it is often convenient to express effective viscosity as a function of second strain rate invariant $\dot{\epsilon}_{\text{II}}^2 = \frac{1}{2}\dot{\epsilon}_{ij}^2$ in form

$$\eta_{\text{eff}} = A_{D1} \frac{1}{(\dot{\epsilon}_{\text{II}}^2)^{(n-1)/2n}} \exp\left(\frac{E_a + V_a P}{nRT}\right) \quad (6.9)$$

where A_{D1} can be calculated on the basis of experimentally determined rheological parameters A_D and n , taking into account type of experiments on which these parameters are based.

For example, in case of axial compression in y direction experiments

$$\dot{\epsilon}_{xx} = \dot{\epsilon}_{zz} = -\frac{1}{2}\dot{\epsilon}_{yy}$$

$$\dot{\epsilon}_{\text{II}}^2 = \frac{1}{2}\dot{\epsilon}_{xx}^2 + \frac{1}{2}\dot{\epsilon}_{yy}^2 + \frac{1}{2}\dot{\epsilon}_{zz}^2 = \frac{3}{4}\dot{\epsilon}_{yy}^2$$

$$\dot{\gamma}_{yy} = -\dot{\epsilon}_{yy}$$

$$\sigma_{xx}' = \sigma_{zz}' = -\frac{1}{2}\sigma_{yy}'$$

$$\sigma_d = \sigma_{xx}' - \sigma_{yy}' = -\frac{3}{2}\sigma_{yy}'$$

$$\sigma_d = \sigma_{xx}' - \sigma_{yy}' = -\frac{3}{2}\sigma_{yy}'$$

$$-\dot{\epsilon}_{yy} = A_D \left(-\frac{3}{2} \sigma_{yy}' \right)^n \exp\left(-\frac{E_a + V_a P}{RT} \right)$$

and thus using

$$2\eta_{eff} \dot{\epsilon}_{yy} = \sigma_{yy}' \text{ and } -\dot{\epsilon}_{yy} = \left(\frac{4}{3} \dot{\epsilon}_{II}^2 \right)^{1/2}$$

we obtain

$$\left(\frac{4}{3} \dot{\epsilon}_{II}^2 \right)^{1/2} = A_D \left(\frac{3}{2} 2\eta_{eff} \left(\frac{4}{3} \dot{\epsilon}_{II}^2 \right)^{1/2} \right)^n \exp\left(-\frac{E_a + V_a P}{RT} \right)$$

$$\eta_{eff} = \left(\frac{1}{2^{(n-1)} 3^{(n+1)/2} A_D} \right)^{1/n} \frac{1}{\left(\dot{\epsilon}_{II}^2 \right)^{(n-1)/2n}} \exp\left(\frac{E_a + V_a P}{nRT} \right)$$

and therefore

$$A_{D1} = \left(\frac{1}{2^{(n-1)} 3^{(n+1)/2} A_D} \right)^{1/n} \quad (6.10)$$

In case of simple xy shear experiments

$$\dot{\epsilon}_{xx} = \dot{\epsilon}_{yy} = \dot{\epsilon}_{zz} = \dot{\epsilon}_{xz} = \dot{\epsilon}_{yz} = 0$$

$$\dot{\epsilon}_{xy} > 0$$

$$\dot{\epsilon}_{II}^2 = \dot{\epsilon}_{xy}^2$$

$$\sigma_d = 2\sigma_{xy}$$

$$\dot{\gamma}_{xy} = 2\dot{\epsilon}_{xy}$$

$$2\dot{\epsilon}_{xy} = A_D (2\sigma_{xy})^n \exp\left(-\frac{E_a + V_a P}{RT} \right)$$

and thus using

$$2\eta_{eff} \dot{\epsilon}_{xy} = \sigma_{xy} \text{ and } \dot{\epsilon}_{xy} = \left(\dot{\epsilon}_{II}^2 \right)^{1/2}$$

we obtain

$$2 \left(\dot{\epsilon}_{II}^2 \right)^{1/2} = A_D \left(4\eta_{eff} \left(\dot{\epsilon}_{II}^2 \right)^{1/2} \right)^n \exp\left(-\frac{E_a + V_a P}{RT} \right)$$

$$\eta_{eff} = \left(\frac{1}{2^{(2n-1)} A_D} \right)^{1/n} \frac{1}{\left(\dot{\epsilon}_{II}^2 \right)^{(n-1)/2n}} \exp\left(\frac{E_a + V_a P}{nRT} \right)$$

and therefore

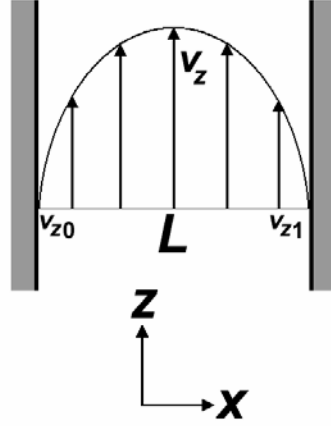
$$A_{D1} = \left(\frac{1}{2^{(2n-1)} A_D} \right)^{1/n} \quad (6.11)$$

Exercise. Please calculate viscosity profile across the 100000 m (100 km) thick mantle lithosphere with temperature linearly increasing from 400°C at the top to 1200 °C in the bottom. Apply conditions

of constant strain rate $(\dot{\epsilon}_{II}^2)^{1/2} = 10^{-14} s^{-1}$. Take the following mantle rheological parameters:

$A_D = 2.5 \times 10^{-17} 1/(Pa^n s)$, $n = 3.5$, $E_a = 532000 J/mol$, $R = 8.313 J/mol$, $V_a = 0$. Take into account that all parameters are based on axial compression experiments.

One of important consequences of *non-Newtonian* rheology of the fluid is that Poisson equation is *not valid* anymore for the uniaxial (e.g., purely vertical) flow of a *non-Newtonian* fluid in a channel and complete Stokes equation has to be used in this case. Let's analyze such non-Newtonian channel flow.



In case of planar channel $v_x=0$, $v_y=0$, $\frac{\partial v_z}{\partial z} = 0$, $\frac{\partial v_z}{\partial y} = 0$ and Stokes equation reduce to

$$\frac{\partial \sigma_{xz}}{\partial x} = \frac{\partial P}{\partial z} - \rho g_z \quad (6.12)$$

Assuming nonlinear relationship between stress and strain rate in form $\dot{\epsilon}_{xz} = A(\sigma_{xz})^n$ Stokes equation can be solved as follows

a) Integrating Stokes equation for stress

$$\sigma_{xz} = \left(\frac{\partial P}{\partial z} - \rho g_z \right) x + C_1, \text{ where } C_1 \text{ is an integration constant}$$

b) Representing stress as a function of strain rate

$$\sigma_{xz} = \left(\frac{\dot{\epsilon}_{xz}}{A} \right)^{1/n}$$

c) Modifying integrated Stokes equation using above equation for stress and relation $\dot{\epsilon}_{xz} = \frac{1}{2} \frac{\partial v_z}{\partial x}$

$$\left(\frac{\dot{\epsilon}_{xz}}{A} \right)^{1/n} = \left(\frac{\partial P}{\partial z} - \rho g_z \right) x + C_1$$

$$\dot{\epsilon}_{xz} = A \left[\left(\frac{\partial P}{\partial z} - \rho g_z \right) x + C_1 \right]^n$$

$$\frac{\partial v_z}{\partial x} = 2A \left[\left(\frac{\partial P}{\partial z} - \rho g_z \right) x + C_1 \right]^n$$

d) Integrating obtained equation for vertical velocity

$$v_z(x) = 2A \frac{\left[\left(\frac{\partial P}{\partial z} - \rho g_z \right) x + C_1 \right]^{n+1}}{(n+1) \left(\frac{\partial P}{\partial z} - \rho g_z \right)} + C_2$$

where C_1 and C_2 are integration constants which can be defined from boundary conditions

For example let's assume the following boundary conditions:

$$v_z(x) = v_{z0} \text{ when } x = 0$$

and

$$\sigma_{xz} = 0 \text{ when } x = L/2 \text{ (} L \text{ is the channel width).}$$

The later condition is equivalent to the condition of symmetric velocity profile

$$v_z(x) = v_{z0} = v_{z1} \text{ when } x = L$$

Then our integration constants become as follows

$$C_1 = - \left(\frac{\partial P}{\partial z} - \rho g_z \right) \frac{L}{2},$$

$$C_2 = v_{z0} - 2A \frac{[C_1]^{n+1}}{(n+1) \left(\frac{\partial P}{\partial z} - \rho g_z \right)}$$

Please, exercise to get above expressions for the integration constants from the specified boundary conditions.

Reading: Turcotte & Schubert, 2002, p. 292-324, Ranalli (1995), chapter 4.4.

LECTURE 8.

Discretisation of continuity and Stokes equations on rectangular grid. Conservative and non-conservative schemes of discretization of Stokes equation. Mechanical boundary conditions and their numerical implementation. No slip, free slip and combined boundary conditions.

Numerical solution of partial differential equations (PDE) requires definition of grid of nodal points within the numerical model. The choice of the grid depends strongly on the type of equations to be solved. *Discretization schemes* for these equations also change with changing type of numerical grid. What types of numerical grid exist in numerical geodynamic modeling?

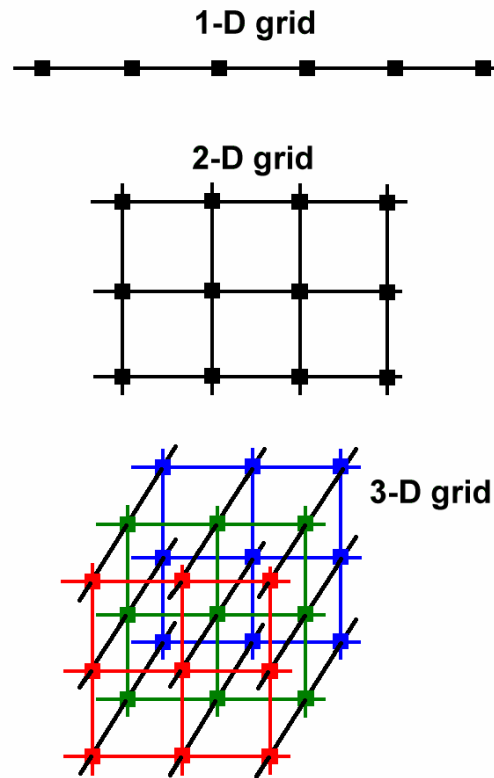


Fig. 8.1. Examples of 1-D, 2-D and 3-D numerical grids.

Depending of the dimension of the problem this grid can be one-, two- and three dimensional (1-D, 2-D, 3-D) (Fig.8.1).

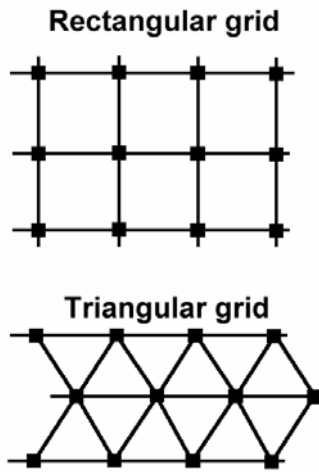


Fig. 8.2. Examples of rectangular and triangular 2-D numerical grids.

Depending on geometry of basic elements the grid can be rectangular and triangular (Fig. 8.2).

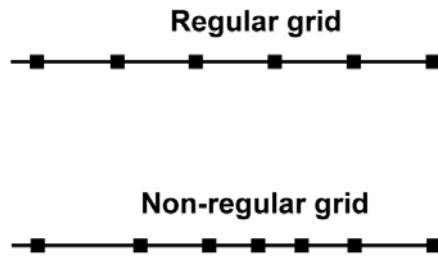


Fig. 8.3. Examples of regular and non-regular 1-D numerical grids.

Depending on the distribution of nodal point the grid can be regular and non-regular (Fig. 8.3).

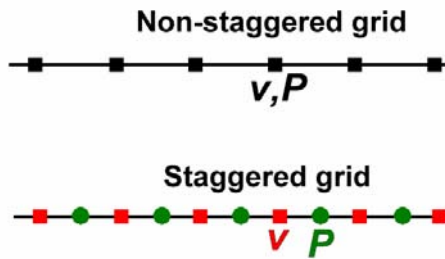


Fig. 8.4. Examples of non-staggered and staggered 1-D numerical grids.

Depending on the character of nodal points the grid can be non-staggered and staggered (half-staggered, fully staggered) (Fig. 8.4).

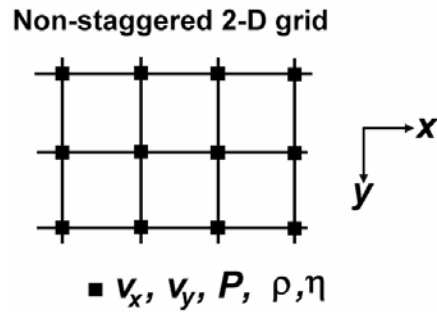


Fig. 8.5. Examples of non-staggered 2-D numerical grid.

Non-staggered grid is the most simple one. All variables for such grid are defined for the same nodes (Fig.8.4, 8.5). In case of using finite-differences (FD) with non-staggered grid all equations are formulated in the same nodal points. Non-staggered grid is natural for solving Poisson equation, heat conservation equation and advective transport equation.

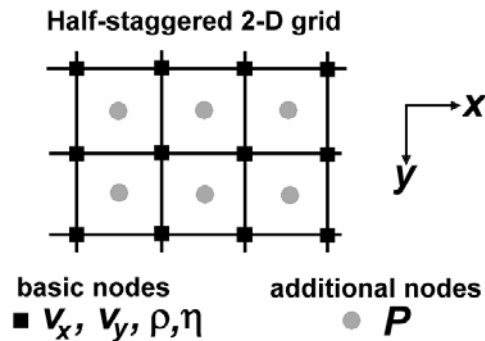


Fig. 8.6. Example of half-staggered 2-D numerical grid.

Half-staggered grid in two dimensions (Fig. 8.6) is a combination of a basic non-staggered grid with an additional set of points defined for the centers of cells formed by the basic grid. Part of variables is then defined in this additional nodes and not in the basic nodal points. Half-staggered grid is natural for solving the combination of Stokes (Poisson) and continuity equations in case of *constant viscosity* when unknown parameters are components of velocity (v_x, v_z) defined in basic nodes and pressure (P) defined in additional nodes (Fig. 8.6). Accordingly, Stokes (Poisson) equations are formulated in basic nodes, though continuity equation is formulated in the additional nodes. Indeed, half-staggered grid is less natural for mechanical and thermomechanical problems with *variable viscosity*.

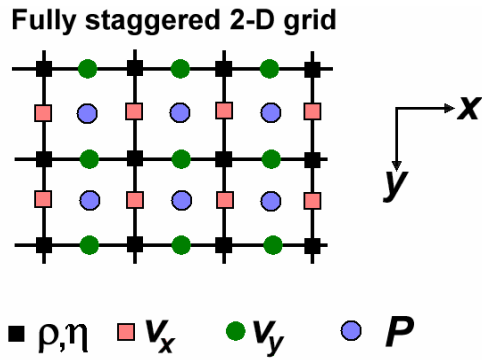


Fig. 8.7. Example of fully staggered 2-D numerical grid.

Fully staggered grid is applied in two and three dimensions and consists of combination of several types of nodal points having different geometrical positions (Fig. 8.7). Different variables are then defined in different nodal points. Different equations are also formulated in different nodal points. Fully staggered grid seems to be the most natural choice in geomodeling for thermomechanical numerical problems with variable viscosity when finite differences are used for solving continuity, Stokes and temperature equations. Discretization of thermomechanical equations on the fully staggered grid is very natural and gives most simple FD formulas. Also, an accuracy of a numerical solution on fully staggered grid is notably (up to four-fold) higher than that on non-staggered grid.

Discretization of equations depends on the type of numerical grid. For example, following discretization schemes can be used for 2-D incompressible continuity equation ($\partial v_x/\partial x + \partial v_y/\partial y = 0$) in case of half-staggered (non-staggered) and fully staggered 2-D grid.

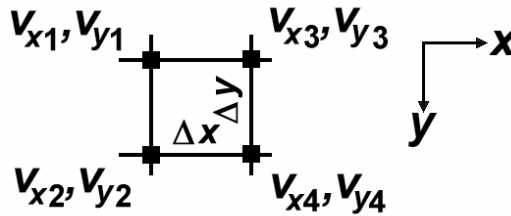


Fig. 8.8. Elementary cell of 2-D non-staggered grid used for discretization of the continuity equation.

Half-staggered (non-staggered) grid (Fig. 8.8):

$$\frac{1}{2}(v_{x3} + v_{x4} - v_{x1} - v_{x2})/\Delta x + \frac{1}{2}(v_{y2} + v_{y4} - v_{y1} - v_{y3})/\Delta y = 0.$$

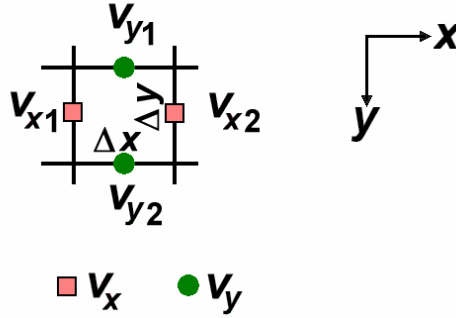


Fig. 8.9. Elementary cell of 2-D fully-staggered grid used for discretization of the continuity equation.

Fully-staggered grid (Fig. 8.9):

$$(v_{x2} - v_{x1})/\Delta x + (v_{y2} - v_{y1})/\Delta y = 0.$$

In both examples continuity equation is formulated for the center of the elementary cell of the grid. However, in case of fully staggered grid resulting formula is more simple and involves less unknowns.

In order to discretize Stokes equation in case of variable viscosity *conservative finite-differences* should be used. Such finite-differences provide conservation of stresses between nodal points allowing correct numerical solution. Below examples of non-conservative and conservative finite-differences for 1-D incompressible Stokes equation ($\partial\sigma'_{xx}/\partial x - \partial P/\partial x = 0$, where $\sigma'_{xx} = 2\eta\partial v_x/\partial x$) are compared for 1-D staggered grid (Fig. 8.10).

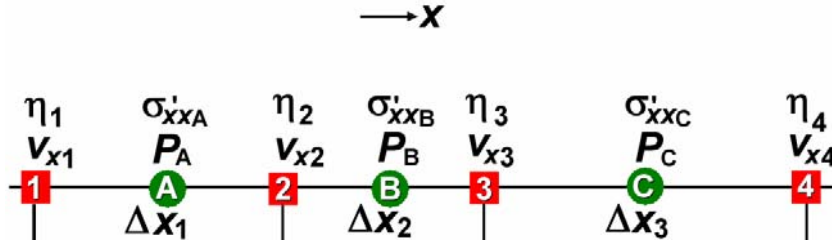


Fig. 8.10. Example of 1-D staggered grid used for discretization of Stokes equation with variable viscosity. 1, 2, 3, 4 - are basic nodes of the grid where Stokes equations are formulated. A, B, C, - are additional (stress) nodes of the grid where stresses are formulated.

Non-conservative FD:

$$\text{node 2: } \{2\eta_2[(v_{x3} - v_{x2})/\Delta x_2 - (v_{x2} - v_{x1})/\Delta x_1] - (P_B - P_A)\}/(\frac{1}{2}\Delta x_1 + \frac{1}{2}\Delta x_2) = 0.$$

$$\text{node 3: } \{2\eta_3[(v_{x4} - v_{x3})/\Delta x_3 - (v_{x3} - v_{x2})/\Delta x_2] - (P_C - P_B)\}/(\frac{1}{2}\Delta x_2 + \frac{1}{2}\Delta x_3) = 0.$$

which implicitly mean that formulations of deviatoric stress σ'_{xxB} for Stokes equations in nodes 2 and 3 are different:

$$\text{node 2: } \sigma'_{xxB} = 2\eta_2(v_{x3} - v_{x2})/\Delta x_2$$

$$\text{node 3: } \sigma'_{xxB} = 2\eta_3(v_{x3} - v_{x2})/\Delta x_2.$$

This implies artificial stress "jumps" between nodes in response of changing viscosity.

Conservative FD:

$$\text{node 2: } \{[(\eta_2+\eta_3)(v_{x3} - v_{x2})/\Delta x_2 - (\eta_1+\eta_2)(v_{x2} - v_{x1})/\Delta x_1] - (P_B - P_A)\}/(\frac{1}{2}\Delta x_1+\frac{1}{2}\Delta x_2) = 0.$$

$$\text{node 3: } \{[(\eta_3+\eta_4)(v_{x4} - v_{x3})/\Delta x_3 - (\eta_2+\eta_3)(v_{x3} - v_{x2})/\Delta x_2] - (P_C - P_B)\}/(\frac{1}{2}\Delta x_2+\frac{1}{2}\Delta x_3) = 0.$$

which means that formulations of deviatoric stress σ_{xxB}' for Stokes equations in nodes 2 and 3 are the same:

$$\sigma_{xxB}' = 2(\eta_2+\eta_3)(v_{x3} - v_{x2})/\Delta x_2.$$

Thus, conservative FD formulation is based on the following three formal rules:

(1) the Stokes equation is initially discretized in term of stress components for *basic nodes* of the grid (cf. nodes 2, 3, Fig. 8.10),

$$\text{node 2: } \{(\sigma_{xxB}' - \sigma_{xxA}') - (P_B - P_A)\}/(\frac{1}{2}\Delta x_1+\frac{1}{2}\Delta x_2) = 0,$$

$$\text{node 3: } \{(\sigma_{xxA}' - \sigma_{xxB}') - (P_C - P_B)\}/(\frac{1}{2}\Delta x_2+\frac{1}{2}\Delta x_3) = 0.$$

(2) these stress components are formulated for *additional (stress) nodes* of the grid (cf. nodes A, B, C, Fig. 8.10)

$$\text{node A: } \sigma_{xxA}' = 2(\eta_1+\eta_2)(v_{x2} - v_{x1})/\Delta x_1,$$

$$\text{node B: } \sigma_{xxB}' = 2(\eta_2+\eta_3)(v_{x3} - v_{x2})/\Delta x_2,$$

$$\text{node C: } \sigma_{xxC}' = 2(\eta_3+\eta_4)(v_{x4} - v_{x3})/\Delta x_3.$$

By averaging viscosity defined in the basic nodes (1, 2, 3, 4) we compute viscosity for the additional nodes (A, B, C) where stress components are defined.

(3) identical formulations of stress components are used for the Stokes equation in different basic nodes.

Applying these rules in 2-D the following conservative formulations can be derived for x- and y-Stokes equations

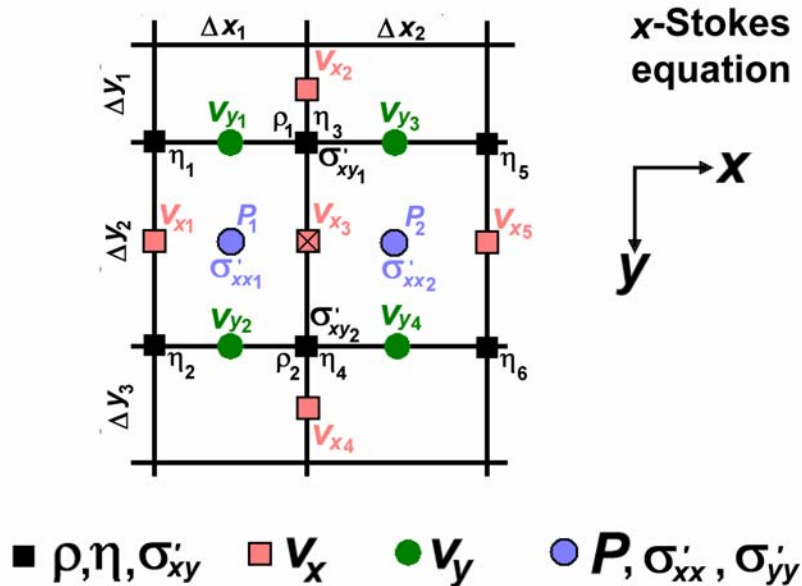


Fig. 8.11. Example of 2-D staggered grid used for discretization of x-Stokes equation with variable viscosity. Crossed red square corresponds to the node for which x-Stokes equation is formulated.

x-Stokes equation (Fig. 8.11):

$$(\sigma_{xy2}' - \sigma_{xy1}')/\Delta y_2 + [(\sigma_{xx2}' - \sigma_{xx1}') - (P_2 - P_1)]/(\frac{1}{2}\Delta x_1 + \frac{1}{2}\Delta x_2) = -\frac{1}{2}(\rho_1 + \rho_2)g_x,$$

where

$$\sigma_{xy1}' = \eta_3[(v_{y2} - v_{y1})/(\frac{1}{2}\Delta x_1 + \frac{1}{2}\Delta x_2) + (v_{x3} - v_{x2})/(\frac{1}{2}\Delta y_1 + \frac{1}{2}\Delta y_2)],$$

$$\sigma_{xy2}' = \eta_4[(v_{y4} - v_{y3})/(\frac{1}{2}\Delta x_1 + \frac{1}{2}\Delta x_2) + (v_{x4} - v_{x3})/(\frac{1}{2}\Delta y_2 + \frac{1}{2}\Delta y_3)],$$

$$\sigma_{xx1}' = \frac{1}{2}(\eta_1 + \eta_2 + \eta_3 + \eta_4)(v_{x3} - v_{x1})/\Delta x_1,$$

$$\sigma_{xx2}' = \frac{1}{2}(\eta_3 + \eta_4 + \eta_5 + \eta_6)(v_{x5} - v_{x3})/\Delta x_2,$$

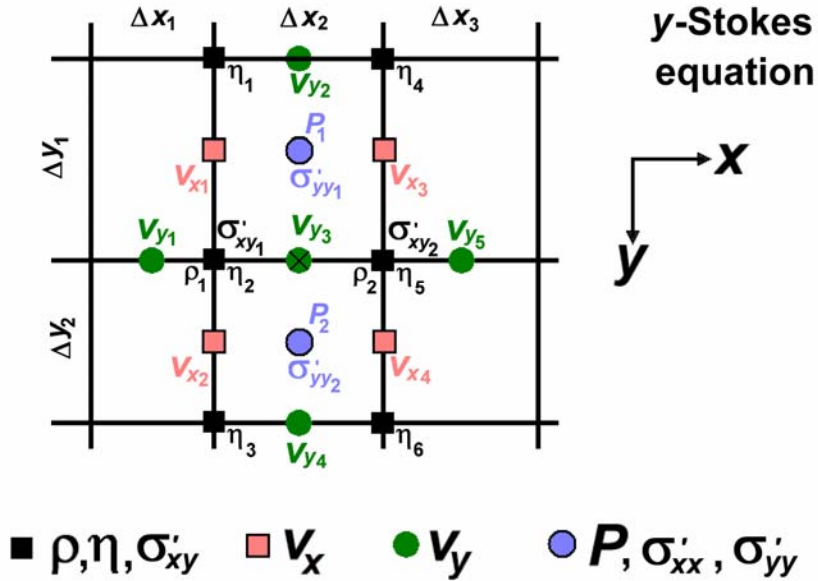


Fig. 8.12. Example of 2-D staggered grid used for discretization of y-Stokes equation with variable viscosity. Crossed green circle corresponds to the node for which y-Stokes equation is formulated.

y-Stokes equation (Fig. 8.12):

$$(\sigma_{xy2}' - \sigma_{xy1}')/\Delta x_2 + [(\sigma_{yy2}' - \sigma_{yy1}') - (P_2 - P_1)]/(\frac{1}{2}\Delta y_1 + \frac{1}{2}\Delta y_2) = -\frac{1}{2}(\rho_1 + \rho_2)g_y,$$

where

$$\sigma_{xy1}' = \eta_2[(v_{x2} - v_{x1})/(\frac{1}{2}\Delta y_1 + \frac{1}{2}\Delta y_2) + (v_{y3} - v_{y1})/(\frac{1}{2}\Delta x_1 + \frac{1}{2}\Delta x_2)],$$

$$\sigma_{xy2}' = \eta_5[(v_{x4} - v_{x3})/(\frac{1}{2}\Delta y_1 + \frac{1}{2}\Delta y_2) + (v_{y5} - v_{y3})/(\frac{1}{2}\Delta x_2 + \frac{1}{2}\Delta x_3)],$$

$$\sigma_{yy1}' = \frac{1}{2}(\eta_1 + \eta_2 + \eta_4 + \eta_5)(v_{y3} - v_{y2})/\Delta y_1,$$

$$\sigma_{yy2}' = \frac{1}{2}(\eta_2 + \eta_3 + \eta_5 + \eta_6)(v_{y4} - v_{y3})/\Delta y_2,$$

In all above examples stress components are formulated via components of strain rate tensor and viscosity according to the general formula $\sigma_{ij}' = 2\eta \dot{\epsilon}_{ij}'$, where $\dot{\epsilon}_{ij}' = \dot{\epsilon}_{ij} - \delta_{ij} \frac{1}{3} \dot{\epsilon}_{kk}$, $\dot{\epsilon}_{ij} = \frac{1}{2} \left(\frac{\partial v_i}{\partial j} + \frac{\partial v_j}{\partial i} \right)$ and $\dot{\epsilon}_{kk} = \dot{\epsilon}_{xx} + \dot{\epsilon}_{yy} + \dot{\epsilon}_{zz} = \text{div}(\bar{v}) = 0$ according to the incompressibility condition.

As we have already seen before, in order to obtain numerical solution boundary conditions have to be defined for the model. Mechanical boundary conditions depend on the type of numerical problem solved. The following boundary conditions are often used in geomodeling:

- (1) no slip,
- (2) free slip,
- (3) free surface,
- (4) fast erosion and
- (5) combined boundary conditions.

No slip condition require all velocity components on the boundary to be zero

$$v_x = v_y = v_z = 0.$$

Free slip condition require normal velocity component on the boundary to be zero and two other components not to change across the boundary. For example for the boundary orthogonal to the x axis free slip condition is formulated as follows

$$v_x = 0,$$

$$\partial v_y / \partial x = \partial v_z / \partial x = 0.$$

Free surface condition require shear stress along the surface to be zero

$$\sigma_{ij}' = 0$$

where i -axis is normal to the surface and $j \neq i$. This condition allows the surface to be deformed.

Fast erosion condition require all velocity components not to change across the boundary. For example for the boundary orthogonal to the x axis fast erosion condition is formulated as follows

$$\partial v_x / \partial x = \partial v_y / \partial x = \partial v_z / \partial x = 0.$$

Numerical implementation of all these boundary conditions depends on the type of the grid. Numerical examples of different boundary conditions are shown below.

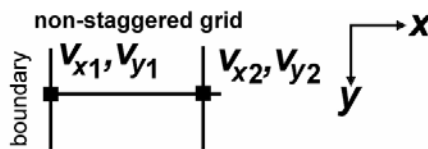


Fig. 8.13. Example of 2-D non-staggered grid used for the formulation of non-slip and free slip boundary conditions.

Non-staggered grid (Fig. 8.13):

no slip - $v_{x1} = 0, v_{y1} = 0$.
 free slip - $v_{x1} = 0, v_{y1} = v_{y2}$.

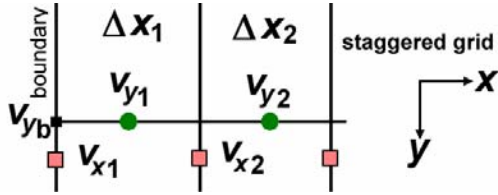


Fig. 8.14. Example of 2-D staggered grid used for the formulation of non-slip and free slip boundary conditions.

Staggered grid (Fig. 8.14):

no slip - $v_{x1} = 0, v_{y1} = v_{y2}[\frac{1}{2}\Delta x_1 / (\Delta x_1 + \frac{1}{2}\Delta x_2)]$,
 free slip - $v_{x1} = 0, v_{y1} = v_{y2}$.

Conditions for the vertical velocity mean that vertical velocity on the boundary v_{yb} (Fig. 8.14) is extrapolated from vertical velocities in two internal nodes according to the formula

$$v_{yb} = v_{y1} + (v_{y1} - v_{y2})[\frac{1}{2}\Delta x_1 / (\frac{1}{2}\Delta x_1 + \frac{1}{2}\Delta x_2)].$$

LECTURE 9.

Heat conduction law. Heat conservation equation and its geodynamic applications. Radioactive, viscous and adiabatic heating and their significance.

After been introduced into mechanical part of numerical geodynamic modeling which is traditionally considered as the most difficult one we now start with thermal modeling. Thermal modeling simulate transport of heat in continuum. Heat transport processes play crucial role in geodynamics and are often inherently coupled to deformation, as for example in case of mantle convection, granitic cupola growth, subduction process, slab breakoff etc. From numerical point of view, heat transport processes are more simple to model. There are, however some numerical difficulties which make subject indeed non-trivial.

Let's first (as usually) study equations which are relevant for heat transport processes. Most basic one is Fourier's law of heat conduction which relate heat flux (q) with temperature gradient $\frac{\partial T}{\partial x}$

$$q = -k \frac{\partial T}{\partial x} \quad (9.1)$$

where k (W m/K) is the thermal conductivity of a material. Thermal conductivity may depend on P, T composition and structure of the material. Heat flux q is an amount of heat passing through the unit surface in unit time. As we all know, heat is always transferred from hot body to the colder one. This is reflected by minus in the right part of Equation (9.1) implying that heat flux is positive in direction of decreasing temperature, i.e. in case when temperature gradient $\frac{\partial T}{\partial x}$ is negative. In three dimensions heat flux is a vector which can be decomposed to three components

$$\underline{q} = (q_x, q_y, q_z)$$

In this case the Fourier's law relates heat fluxes in different directions with respective temperature gradients

$$q_i = -k \frac{\partial T}{\partial i} \quad (9.2)$$

or

$$q_x = -k \frac{\partial T}{\partial x}, \quad q_y = -k \frac{\partial T}{\partial y}, \quad q_z = -k \frac{\partial T}{\partial z},$$

where i is coordinate (x, y, z).

In order to predict changes in temperature due to the heat transport *heat conservation equation* also called *temperature equation* has to be solved. This equation describes balance of heat in continuum and relates temperature changes with internal heat generation as well as *advective* and *conductive* heat transport. Lagrangian temperature equation has the following form

$$\rho C_p \frac{DT}{Dt} = -\frac{\partial q_i}{\partial i} + Hr + Hs + Ha \quad (9.3)$$

or writing in complete 3-D form

$$\rho C_p \frac{DT}{Dt} = -\frac{\partial q_x}{\partial x} - \frac{\partial q_y}{\partial y} - \frac{\partial q_z}{\partial z} + Hr + Hs + Ha,$$

or using relation (9.2)

$$\rho C_p \frac{DT}{Dt} = \frac{\partial}{\partial x} \left(k \frac{\partial T}{\partial y} \right) + \frac{\partial}{\partial y} \left(k \frac{\partial T}{\partial x} \right) + \frac{\partial}{\partial z} \left(k \frac{\partial T}{\partial z} \right) + Hr + Hs + Ha$$

where index i , thus, means *summation* of derivatives of heat flux components by respective coordinates (x, y, z) ; ρ is density (kg/m^3); C_p is isobaric heat capacity (J/kg/K); Hr , Hs and Ha are respectively radioactive, shear and adiabatic heat productions (W/m^3). $\frac{DT}{Dt}$ is substantive time derivative of temperature corresponding to the standard Lagrangian-Eulerian relation that we have already discussed in Lectures 3 and 5

$$\frac{DT}{Dt} = \frac{\partial T}{\partial t} + \bar{v} \times \text{grad}(T).$$

For example, in 3-D

$$\frac{DT}{Dt} = \frac{\partial T}{\partial t} + v_x \frac{\partial T}{\partial x} + v_y \frac{\partial T}{\partial y} + v_z \frac{\partial T}{\partial z}.$$

Accordingly, in Eulerian form temperature equation can be written as follows

$$\rho C_p \left(\frac{\partial T}{\partial t} + \bar{v} \times \text{grad}(T) \right) = -\frac{\partial q_i}{\partial i} + Hr + Hs + Ha \quad (9.4)$$

or writing in complete 3-D form

$$\rho C_p \left(\frac{\partial T}{\partial t} + v_x \frac{\partial T}{\partial x} + v_y \frac{\partial T}{\partial y} + v_z \frac{\partial T}{\partial z} \right) = -\frac{\partial q_x}{\partial x} - \frac{\partial q_y}{\partial y} - \frac{\partial q_z}{\partial z} + Hr + Hs + Ha$$

or using relation (9.2)

$$\rho C_p \left(\frac{\partial T}{\partial t} + v_x \frac{\partial T}{\partial x} + v_y \frac{\partial T}{\partial y} + v_z \frac{\partial T}{\partial z} \right) = \frac{\partial}{\partial x} \left(k \frac{\partial T}{\partial y} \right) + \frac{\partial}{\partial y} \left(k \frac{\partial T}{\partial x} \right) + \frac{\partial}{\partial z} \left(k \frac{\partial T}{\partial z} \right) + Hr + Hs + Ha$$

There are several type of heat generation/consumption processes that are taken into account in the temperature equation. *Radioactive heat production* (Hr) is due to the decay of radioactive elements always present in rocks. It strongly depends on the type of rocks and typical values are: $2 \times 10^{-6} \text{ W/m}^3$ for granites, $2.5 \times 10^{-7} \text{ W/m}^3$ for basalts and $2 \times 10^{-8} \text{ W/m}^3$ for mantle rocks. *Shear heat production* (Hs) is related to the dissipation of mechanical energy during irreversible (e.g., viscous) deformation and can be calculated via deviatoric stresses and strain rates as follows

$$Hs = \sigma_{ij}' \dot{\epsilon}_{ij}' \quad (9.5)$$

where i and j are coordinates (x, y, z) and ij denotes summation. In case of 3-D viscous deformation

$$Hs = \sigma_{xx}' \dot{\epsilon}_{xx}' + \sigma_{yy}' \dot{\epsilon}_{yy}' + \sigma_{zz}' \dot{\epsilon}_{zz}' + 2(\sigma_{xy}' \dot{\epsilon}_{xy}' + \sigma_{xz}' \dot{\epsilon}_{xz}' + \sigma_{yz}' \dot{\epsilon}_{yz}')$$

Adiabatic heat production/consuming (*adiabatic heating/cooling*) is related to changes in pressure and can be calculated via pressure changes as follows

$$Ha = T \alpha \frac{DP}{Dt}, \quad (9.6)$$

where $\frac{DP}{Dt}$ is substantive time derivative of pressure. In contrast to shear and radioactive heating adiabatic effects can be either positive or negative. As it is well known from thermodynamics

temperature of a substance under conditions of no thermal exchange increases with increasing pressure and decreases with decreasing pressure thus directly reflecting sign of $\frac{DP}{Dt}$. Effects of adiabatic heating can be very significant in case of strong changes in pressure which has strong implication for the mantle convection process.

In complete form temperature equation looks quite complicated, but at least it does not "hide" three equations in one in contrast to the momentum equation... In case of constant thermal conductivity $k=const$ temperature equation simplify to

$$\rho C_p \frac{DT}{Dt} = k \frac{\partial^2 T}{\partial x^2} + k \frac{\partial^2 T}{\partial y^2} + k \frac{\partial^2 T}{\partial z^2} + Hr + Hs + Ha \quad (9.7)$$

or

$$\rho C_p \frac{DT}{Dt} = k \Delta T + Hr + Hs + Ha$$

where $\Delta = \frac{\partial^2}{\partial x^2} + \frac{\partial^2}{\partial y^2} + \frac{\partial^2}{\partial z^2}$ is *Laplace operator*, which is common abbreviation used in continuum mechanics.

When internal heat production is negligible and there is no advection of material (purely conductive heat transport) temperature equation take the form similar to Poisson equation

$$\frac{\partial T}{\partial t} = \kappa \Delta T ,$$

where $\kappa = k/(\rho C_p)$ is thermal diffusivity (m^2/sec).

When temperature does not change with time then heat conservation is described by the steady temperature equation. Steady Eulerian temperature equation $\frac{\partial T}{\partial t} = 0$ corresponds to the case when temperature remains constant in immobile Eulerian observation points while temperature in Lagrangian points can change. In this case temperature equation is as follows.

$$\rho C_p (\bar{v} \times grad(T)) = -\frac{\partial q_i}{\partial i} + Hr + Hs + Ha . \quad (9.8)$$

This form of equation is often used for computing of equilibrium temperature profiles across deforming medium, for example in case of steady magma flow in a channel. Steady Lagrangian temperature equation $\frac{DT}{Dt} = 0$ corresponds to the case when temperature does not change in

Lagrangian points but can vary in Eulerian observation points according to the purely advective heat transport

$$\frac{DT}{Dt} = \frac{\partial T}{\partial t} + \bar{v} \times grad(T) = 0 . \quad (9.9)$$

or

$$\frac{\partial T}{\partial t} = -\bar{v} \times grad(T)$$

In this case temperature equation is as follows

$$-\frac{\partial q_i}{\partial i} + Hr + Hs + Ha = 0$$

Steady Eulerian-Lagrangian temperature equation ($\frac{\partial T}{\partial t} = 0$ and $\frac{DT}{Dt} = 0$) holds for the case when no displacement of medium occur and therefore $Hs=0$ and $Ha=0$. This equation has most simple form

$$-\frac{\partial q_i}{\partial i} + Hr = 0 \quad (9.10)$$

and is often used for the calculation of steady geotherms characterising changes of temperature with depth in the layered sequence of rocks with variable radioactive heat production.

Exercise. Please, integrate Equation (9.10) to calculate steady temperature profile across the continental crust with radioactive heat production $Hr=1 \times 10^{-6} \text{ W/m}^3$, if temperature at the surface is 300 K and temperature in the bottom of the crust is 700 K. Take thermal conductivity of the crust to be 2 W/(m K).

Non steady temperature profiles can be calculated in 1-D case using Fourier series expansion. For example calculations can be done for the flow of viscous fluid with constant viscosity η in a vertical channel. Boundary conditions are taken as follows: given vertical pressure gradient, $\partial P/\partial z$, along the channel, non-slip conditions and $T=\text{const}$ and $\partial T/\partial z=\text{const}$ at the walls. The initial conditions are $T=T_0$ and $\partial T/\partial x=0$.

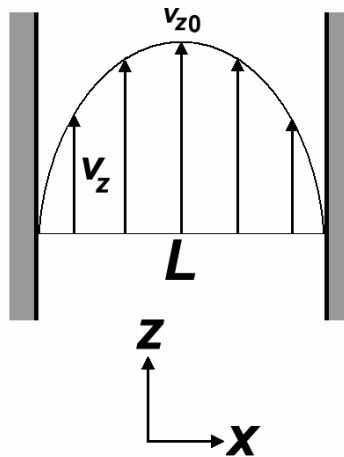


Figure. 9.1. Planar flow of viscous fluid in the channel.

The horizontal steady-state profile for vertical velocities, v_z , is defined by the equation (see Lecture 6)

$$v_z = 4v_{z0}(Lx - x^2)/L^2,$$

$$v_{z0} = -L^2(\partial P/\partial z)/(8\eta),$$

where L is the width of the channel; η is the viscosity of the channel; v_{z0} is the vertical velocity in the centre of the channel.

General form of non-steady 1-D solution is given in textbooks.

The corresponding temperature changes in the channel as a function of time are given by the following series expansion

$$\Delta T(x, t) = \sum_{m=1}^{\infty} F_m E_{mt} \sin[\pi(2m-1)x/L],$$

where

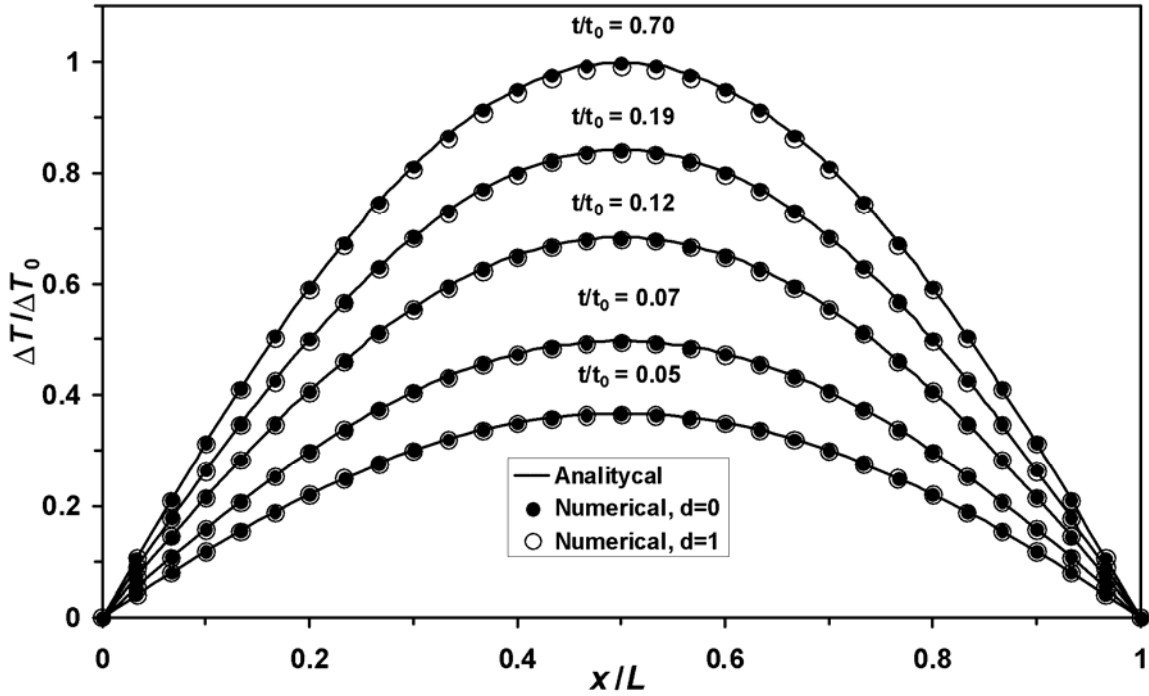
$$F_m = -8\xi L^2 / [\pi(2m-1)]^3,$$

$$E_{mt} = L^2 / [\pi(2m-1)]^2 \{1 - \exp(-[\pi(2m-1)/L]^2 \kappa t)\} / \kappa,$$

$$\kappa = k / (\rho C p),$$

$$\xi = 4v_{z0} / L^2 (\partial T_o / \partial z),$$

where $\Delta T(x, t)$ is the temperature in the channel as a function of the spatial coordinates and time; κ is a constant thermal diffusivity in $\text{m}^2 \cdot \text{s}^{-1}$. When calculating analytical solution an infinite summation of series expansion can be cut after $m=20$ due to negligible contribution of members of higher order. Above equation does not account for shear and adiabatic heating. This equation can be used for benchmarking of non steady numerical solution for the heat transport.

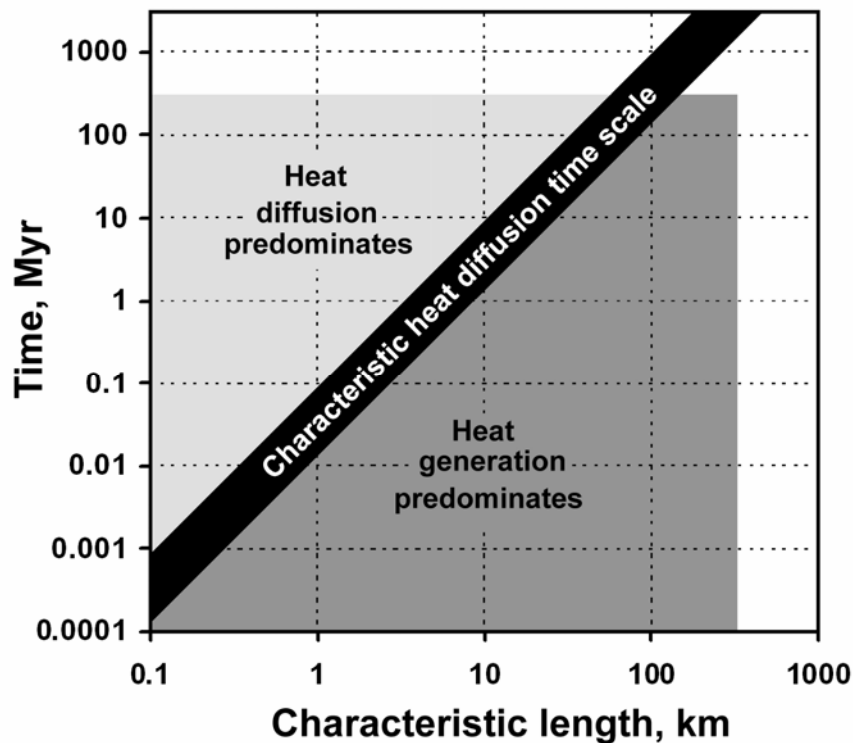


The non-steady temperature changes within the Newtonian channel flow. $t_0 = L^2 / \kappa$ is characteristic thermal diffusion timescale, $\Delta T_0 = 5v_{z0}(\partial T_o / \partial z) \rho C p L^2 / (48k)$ is maximal temperature change in the center of the channel corresponding to the final steady temperature profile given by Eq. 9.8.

Another important aspect that can be analysed analytically concerns *time scale* of heat conduction process. Heat generated within any region is spread by conduction with a characteristic time scale (t_0) that depends on the width L of the region

$$t_0 = \frac{L^2}{\kappa}$$

Therefore, the duration of heat dissipation via conduction grows as the square of the width (L) of the region. For instance, though the shear heat produced within a 100 meter wide shear zone dissipates in only ~1000 yr, the heat generated within a 1 km wide shear zone requires about 100,000 yr for the similar degree of conductive cooling.



Timescales for different thermal regimes calculated according to equation $t_0 = \frac{L^2}{\kappa}$ with $\kappa = 10^{-6} \text{ m}^2\text{s}^{-1}$.

Shaded areas show lengths and timescales characteristic of collisional orogens.

Reading: Turcotte & Schubert, 2002, p. 132-171.

LECTURE 10.

Discretization of heat conservation equation using finite differences. Conservative and non-conservative schemes of discretization. Explicit and implicit schemes of numerical solving of heat conservation equation. Advective terms: upwind differences, numerical diffusion, Lagrangian methods. Thermal boundary conditions: constant temperature, constant heat flow, combined conditions. Numerical implementation of thermal boundary conditions.

We now start with numerical representation and solving of the temperature equation. Discretization of temperature equation with finite differences can be *explicit* and *implicit*. In order to understand the difference let us consider an example. Most simple discretization can be done for the temperature equation describing heat diffusion in a non-deforming medium with constant thermal conductivity (k), density (ρ), heat capacity (C_p) and thus constant thermal diffusivity $\kappa = k/(\rho C_p)$:

$$\frac{\partial T}{\partial t} = \frac{k}{\rho C_p} \Delta T \quad (10.1).$$

In 2-D case this discretization is as follow

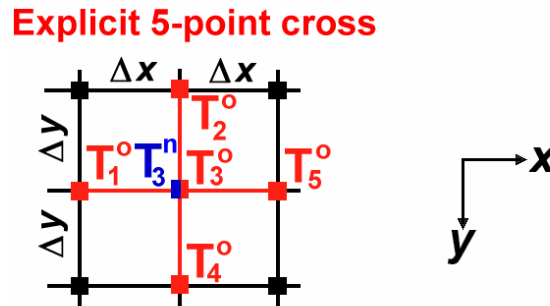


Figure. 10.1. Example of 2-D numerical grid for explicit discretization of the temperature equation with constant thermal diffusivity.

Explicit FD (Fig. 10.1):

$$\frac{T_3^n - T_3^o}{\Delta t} = \frac{k}{\rho C_p} \left(\frac{T_1^o - 2T_3^o + T_5^o}{\Delta x^2} + \frac{T_2^o - 2T_3^o + T_4^o}{\Delta y^2} \right).$$

This form is called explicit because new temperature (T^n) for the next time instant t_n can be explicitly calculated from the temperatures (T^o) known for the current time instant t_o ($t_n = t_o + \Delta t$, where Δt is time step):

$$T_3^n = \frac{k\Delta t}{\rho C_p} \left(\frac{T_1^o - 2T_3^o + T_5^o}{\Delta x^2} + \frac{T_2^o - 2T_3^o + T_4^o}{\Delta y^2} \right) + T_3^o.$$

Explicit formulation has strong limitation for the time step $\Delta t < \Delta x^2/(3\kappa)$. Larger time steps produce oscillations of numerical solution growing with time (Fig. 10.2). One can also see examples of these oscillations by using exercise MatLab program called explicit.m for this lecture.

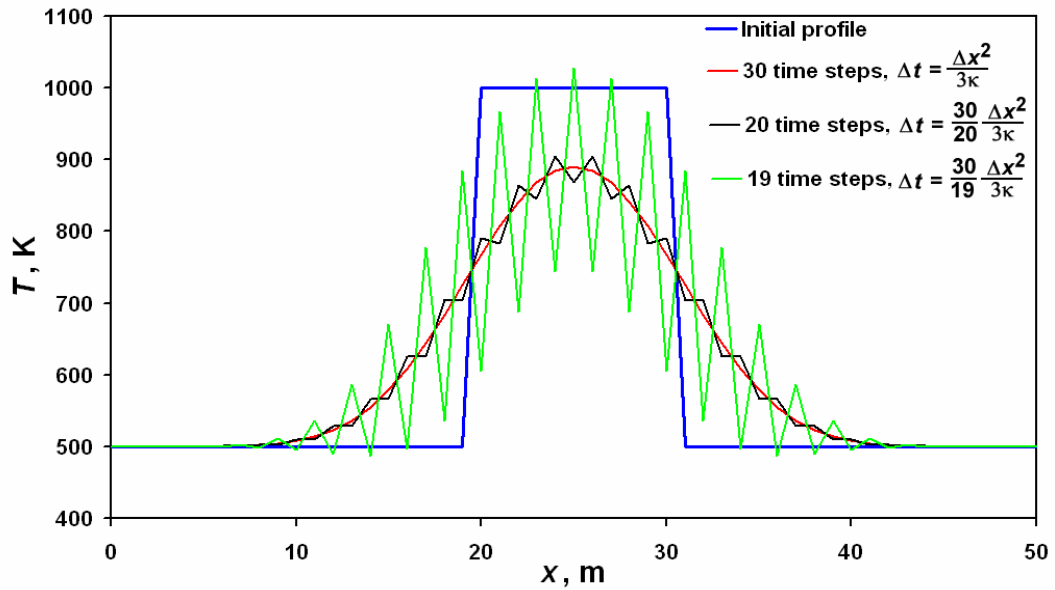


Figure. 10.2. Oscillations of explicit numerical solution of equation (10.1) due to the large time step.

Implicit 5-point cross

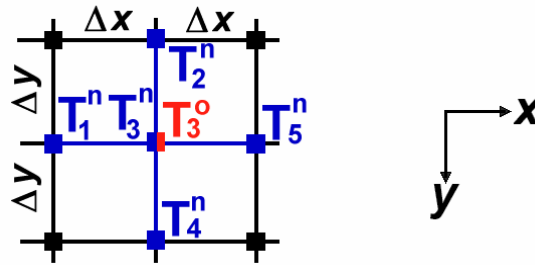


Figure. 10.3. Example of 2-D numerical grid for explicit discretization of the temperature equation with constant thermal diffusivity.

Implicit FD (Fig. 10.3):

$$\frac{T_3^n - T_3^o}{\Delta t} = \frac{k}{\rho C p} \left(\frac{T_1^n - 2T_3^n + T_5^n}{\Delta x^2} + \frac{T_2^n - 2T_3^n + T_4^n}{\Delta y^2} \right).$$

This form is called implicit because new temperature (T^n) for the next time instant t_n can not be explicitly calculated from the temperatures (T^o) known for the current time instant. In order to obtain new temperatures the system of equations written for all points of the model have to be solved:

$$\frac{T_3^n}{\Delta t} - \frac{k}{\rho C p} \left(\frac{T_1^n - 2T_3^n + T_5^n}{\Delta x^2} + \frac{T_2^n - 2T_3^n + T_4^n}{\Delta y^2} \right) = \frac{T_3^o}{\Delta t}.$$

It is important to mention that the implicit formulation has no limitation for the time step.

In case of discretization of heat conservation equation for numerical problems with variable thermal conductivity (k) conservative finite-differences should be used. Such finite-differences provide conservation of heat fluxes between nodal points allowing correct numerical solution. In a

general sense, this is analogous to the formulation of conservative finite differences for Stokes equation with variable viscosity which we studied in Lecture 4. Below examples of non-conservative and conservative finite-differences for 1-D heat conservation equation $\rho C_p \frac{DT}{Dt} = -\frac{\partial q_x}{\partial x}$, where $q_x = -k \frac{\partial T}{\partial x}$ are compared (Fig. 10.4).

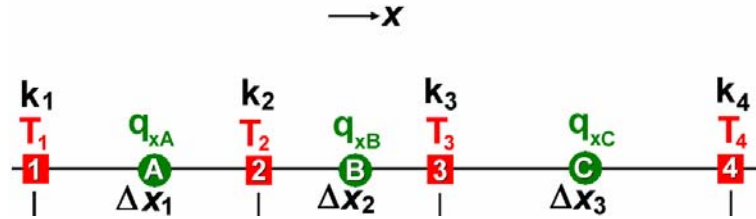


Figure. 10.4. Example of 1-D staggered grid used for discretization of temperature equation with variable thermal conductivity. 1, 2, 3, 4 - are basic nodes of the grid where Stokes equations are formulated. A, B, C, - are additional (heat flux) nodes of the grid where stresses are formulated.

Non-conservative FD:

$$\text{node 2: } \left(\rho C_p \frac{DT}{Dt} \right)_2 = - \left(\frac{\partial q_x}{\partial x} \right)_2 \text{ where } \left(\frac{\partial q_x}{\partial x} \right)_2 = -k_2 \frac{\frac{T_3 - T_2}{\Delta x_2} - \frac{T_2 - T_1}{\Delta x_1}}{2}$$

$$\text{node 3: } \left(\rho C_p \frac{DT}{Dt} \right)_3 = - \left(\frac{\partial q_x}{\partial x} \right)_3 \text{ where } \left(\frac{\partial q_x}{\partial x} \right)_3 = -k_3 \frac{\frac{T_4 - T_3}{\Delta x_3} - \frac{T_3 - T_2}{\Delta x_2}}{2}$$

which implicitly mean that formulations of horizontal heat flux q_{xB} for temperature equations in nodes 2 and 3 are different:

$$\text{node 2: } q_{xB} = -k_2(T_3 - T_2)/\Delta x_2$$

$$\text{node 3: } q_{xB} = -k_3(T_3 - T_2)/\Delta x_2.$$

This implies artificial heat flux "jumps" between basic nodes in response of changing thermal conductivity

Conservative FD (write complete temperature equations ???)

$$\rho C_p \frac{DT}{Dt} = -\frac{\partial q_x}{\partial x}$$

$$\text{node 2: } \left(\rho C_p \frac{DT}{Dt} \right)_2 = - \left(\frac{\partial q_x}{\partial x} \right)_2,$$

$$\text{where } \left(\frac{\partial q_x}{\partial x} \right)_2 = \frac{q_{xB} - q_{xA}}{(\Delta x_2 + \Delta x_1)/2} \text{ or } \left(\frac{\partial q_x}{\partial x} \right)_2 = -\frac{\frac{(k_2 + k_3)(T_3 - T_2)}{2\Delta x_2} - \frac{(k_1 + k_2)(T_2 - T_1)}{2\Delta x_1}}{(\Delta x_1 + \Delta x_2)/2}$$

$$\text{node 3: } \left(\rho C p \frac{DT}{Dt} \right)_3 = - \left(\frac{\partial q_x}{\partial x} \right)_3,$$

$$\text{where } \left(\frac{\partial q}{\partial x} \right)_2 = \frac{q_{xB} - q_{xA}}{(\Delta x_2 + \Delta x_1)/2} \quad \text{or} \quad \left(\frac{\partial q}{\partial x} \right)_3 = - \frac{\frac{(k_3 + k_4)(T_4 - T_3)}{2\Delta x_3} - \frac{(k_2 + k_3)(T_3 - T_2)}{2\Delta x_2}}{\frac{(\Delta x_2 + \Delta x_3)}{2}}$$

which means that formulations of heat flux q_{xB} for temperature equations in nodes 2 and 3 are the same:

$$q_{xB} = (k_2 + k_3)(T_3 - T_2)/\Delta x_2.$$

Effective thermal conductivity for node B is, thus, calculated as an arithmetic mean of conductivities for nodes 1 and 2. Another possibility is to use a harmonic mean

$$q_{xB} = 2k_2k_3/(k_2 + k_3)(T_3 - T_2)/\Delta x_2.$$

This formula follows from the condition of equal heat fluxes to the left and to the right of the node B *under assumption* that heat conductivities between nodes 2 and B and B and 3 remain constant and are equal to k_2 and k_3 , respectively. Then the following formulas can be written

$$q_{xB} = k_2(T_B - T_2)/2\Delta x_2 \quad (10.2)$$

$$q_{xB} = k_3(T_3 - T_B)/2\Delta x_2 \quad (10.3)$$

$$q_{xB} = k_B(T_3 - T_2)/\Delta x_2 \quad (10.4)$$

where $k_B = 2k_2k_3/(k_2 + k_3)$ and $T_B = (T_2k_2 + T_3k_3)/(k_2 + k_3)$ are effective thermal conductivity and temperature for the node B, respectively.

Exercise. Please derive formulas for k_B and T_B by using conditions (10.2)-(10.4).

To summarize, conservative FD formulation is based on the following three formal rules which are analogous to the rules discussed in Lecture 8 for the Stokes equation with variable viscosity.

(1) the temperature equation is initially discretized in term of heat fluxes for *basic nodes* of the grid (cf. nodes 2, 3, Fig. 10.4),

$$\text{node 2: } [\rho C p (DT/Dt)]_2 = -(q_{xB} - q_{xA})(\frac{1}{2}\Delta x_1 + \frac{1}{2}\Delta x_2),$$

$$\text{node 3: } [\rho C p (DT/Dt)]_3 = -(q_{xC} - q_{xB})(\frac{1}{2}\Delta x_2 + \frac{1}{2}\Delta x_3).$$

(2) these heat fluxes are formulated for *additional (heat flux) nodes* of the grid (cf. nodes A, B, C, Fig. 10.4)

$$\text{node A: } q_{xA} = (k_1 + k_2)(T_2 - T_1)/2\Delta x_1,$$

$$\text{node B: } q_{xB} = (k_2 + k_3)(T_3 - T_2)/2\Delta x_2.,$$

$$\text{node C: } q_{xC} = (k_3 + k_4)(T_4 - T_3)/2\Delta x_3.$$

By averaging thermal conductivity defined in the basic nodes (1, 2, 3, 4) we compute conductivity for the additional nodes (A, B, C) where heat fluxes are defined.

(3) identical formulations of heat fluxes are used for the temperature equation in different basic nodes.

It is important to mention that conservative finite differences are formulated *in term of heat conductivity (k) and not in term of thermal diffusivity $\kappa = k/(\rho Cp)$* , otherwise one can obtain artificial variations in heat fluxes due to variations in density (ρ) and heat capacity (Cp). Both density and heat capacity should be placed in the left part of the temperature equation and taken from the basic node where this equation is formulated.

Applying these rules in 2-D the following conservative formulations can be derived for the temperature equation (Fig. 10.5)

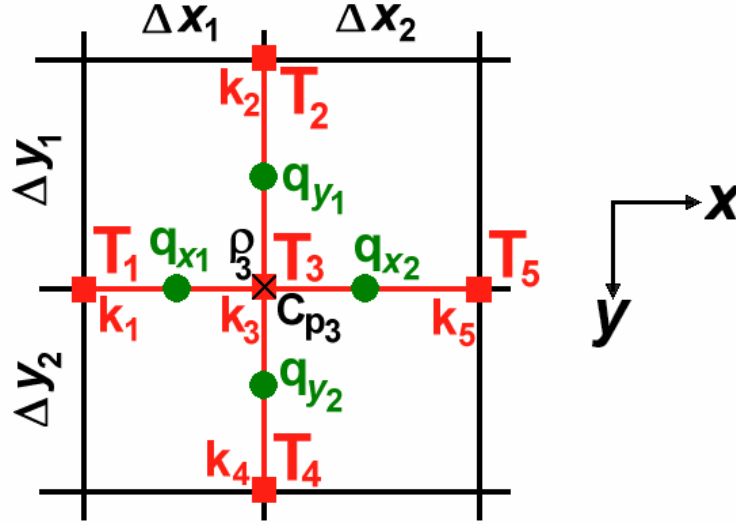


Figure. 10.5. Example of 2-D grid used for discretization of the temperature equation with variable thermal conductivity. Crossed red rectangle corresponds to the node for which the temperature equation is formulated.

$$\left(\frac{DT}{\partial t}\right) = \frac{1}{\rho_3 Cp_3} \left(-\frac{q_{x2} - q_{x1}}{(\Delta x_2 + \Delta x_1)/2} - \frac{q_{y2} - q_{y1}}{(\Delta y_2 + \Delta y_1)/2} \right),$$

where

$$q_{x1} = -\frac{(k_1 + k_3)(T_3 - T_1)}{2 \cdot 2\Delta x_1},$$

$$q_{x2} = -\frac{(k_3 + k_5)(T_5 - T_3)}{2 \cdot \Delta x_2},$$

$$q_{y1} = -\frac{(k_2 + k_3)(T_3 - T_2)}{2 \cdot 2\Delta y_1},$$

$$q_{y2} = -\frac{(k_3 + k_4)(T_4 - T_3)}{2 \cdot \Delta y_2}.$$

Obviously, conservative formulation can either be explicit or implicit.

If advective term is present in the Eulerian temperature equation it should also be included in FD formulation

$$\rho C_p \left(\frac{\partial T}{\partial t} + \bar{v} \times \text{grad}(T) \right) = -\frac{\partial q_i}{\partial i}$$

In this case explicit FD involving temperature and velocity from the current time instant are most often used. Common approach is to use asymmetric "upwind" differences, i.e. take FD against the direction of material flow vector:

Explicit 5-point cross

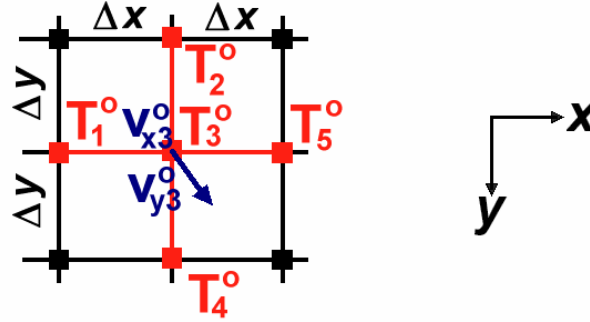


Figure. 10.6. Example of 2-D grid used for discretization of the advective term for the Eulerian temperature equation.

$$\bar{v}_3 \times \text{grad}(T)_3 = v_{x3} \left(\frac{\partial T}{\partial x} \right)_3 + v_{y3} \left(\frac{\partial T}{\partial y} \right)_3$$

Explicit upwind differences are then as follows

$$\bar{v}_3 \times \text{grad}(T)_3 = v_{x3}^o \left(\frac{\partial T^o}{\partial x} \right)_3 + v_{y3}^o \left(\frac{\partial T^o}{\partial y} \right)_3$$

$$\left(\frac{\partial T^o}{\partial x} \right)_3 = \frac{T_3^o - T_1^o}{\Delta x} \text{ when } v_{x3}^o > 0 \text{ and } \left(\frac{\partial T^o}{\partial x} \right)_3 = \frac{T_5^o - T_3^o}{\Delta x} \text{ when } v_{x3}^o < 0$$

$$\left(\frac{\partial T^o}{\partial y} \right)_3 = \frac{T_3^o - T_2^o}{\Delta y} \text{ when } v_{y3}^o > 0 \text{ and } \left(\frac{\partial T^o}{\partial y} \right)_3 = \frac{T_4^o - T_3^o}{\Delta y} \text{ when } v_{y3}^o < 0.$$

Independent on either explicit or implicit formulation, advective terms with variable velocity always introduce (non physical) *numerical diffusion* of temperature on the Eulerian grid. This problem is not relevant for slow flows because real diffusion is much faster than the numerical diffusion. Numerical diffusion becomes relevant for models with rapid advection (e.g. for models of subduction process). This problem can be minimized: (i) by using more complicated Eulerian advection FD schemes, (ii) by advecting temperature with Lagrangian points (method of characteristics, method of markers).

In order to solve temperature equation numerically thermal boundary conditions have to be specified. These conditions depend on the type of numerical problem solved. The following boundary conditions are often used in geomodeling:

constant temperature,
 no heat flux,
 constant heat flux and
 combined boundary conditions.

Numerical examples of different boundary conditions are shown below (Fig. 10.7).

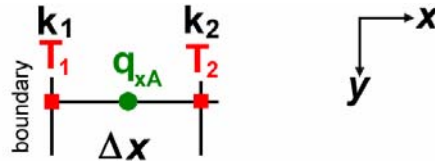


Figure. 10.7. Example of 2-D grid used for discretization of thermal boundary conditions.

constant temperature: $T_1 = \text{const}$, or in standard linear form $1 \times T_1 = \text{const}$

no heat flux: $T_1 = T_2$, or in standard linear form $1 \times T_1 + (-1) \times T_2 = 0$

constant heat flux: $q_{xA} = -\frac{1}{2}(k_1+k_2) \times (T_2 - T_1) / \Delta x = \text{const}$, or $[\frac{1}{2}(k_1+k_2) / \Delta x] \times T_1 + [-\frac{1}{2}(k_1+k_2) / \Delta x] \times T_2 = \text{const}$.

LECTURE 11.

Advection equation. Methods of solving for continuous and discontinuous variables. Marker-in-cell method for solving advection equation. Runge-Kutta advection schemes. Numerical interpolation schemes between markers and nodes.

Advection equation is used to change distribution of physical properties of deforming continuum with time. For a scalar value (A) in Eulerian point this equation can be written as follows

$$\frac{\partial A}{\partial t} = -v_x \left(\frac{\partial A}{\partial x} \right) - v_y \left(\frac{\partial A}{\partial y} \right) - v_z \left(\frac{\partial A}{\partial z} \right).$$

For Lagrangian point the following advection equation relates changes in its coordinates (x, y, z) with material velocities (v_x, v_y, v_z).

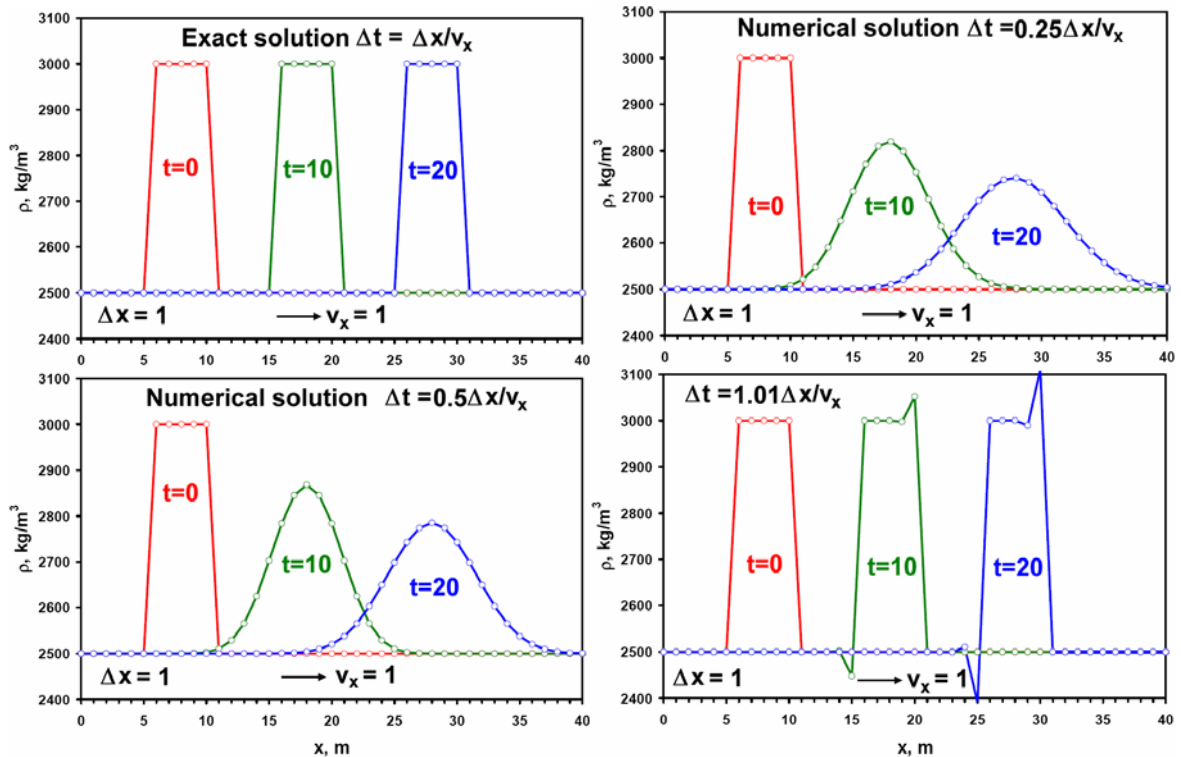
$$\frac{\partial x}{\partial t} = v_x$$

$$\frac{\partial y}{\partial t} = v_y$$

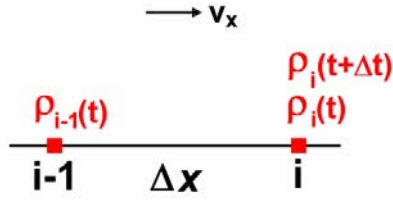
$$\frac{\partial z}{\partial t} = v_z$$

Advection equations look trivial but it is an apparent simplicity. Their numerical solving often causes problems. One of the problems is numerical diffusion of sharp gradients during advection. The following figure demonstrate how sharp density step is smoothed out (diffuses) during numerical solving of 1D advection equation.

$$\frac{\partial \rho}{\partial t} = -v_x \left(\frac{\partial \rho}{\partial x} \right)$$



The equation is solved on the regular Eulerian 1D grid with constant distance between nodes ($\Delta x=1$) for the case of constant material velocity ($v_x=1$) and constant time step ($\Delta t = 0.5 = \frac{1}{2}\Delta x/v_x$) by applying upwind differences



$$\rho_i(t + \Delta t) = \rho_i(t) - v_x \Delta t \frac{\rho_i(t) - \rho_{i-1}(t)}{\Delta x}$$

The rate of numerical diffusion depends on the amount of numerical steps and not on the length of numerical steps. Therefore smaller timestep gives more diffusion. On the other hand for the stability of numerical solution time step should be sufficiently small to make sure that condition

$$v_x \Delta t \leq \Delta x$$

is satisfied in every Eulerian point (otherwise solution starts to oscillate).

In geomodeling an advection of non-diffusive properties (e.g., density) with discontinuous (e.g., step-like) distribution these properties is often needed. One of the most popular methods in this case is the using of Lagrangian points: method of markers (tracers, characteristics) for advection of physical properties. These properties are initially distributed on large amount of Lagrangian point which are passively moved according to a computed velocity field. Material properties on the Eulerian grid are then interpolated from the displaced Lagrangian points. This is so called marker-in-cell technique.

To move a Lagrangian point (A) different advection schemes can be used. Most simple is the first order of accuracy advection scheme

$$x_A(t + \Delta t) = x_A(t) + v_{xA}(t) \Delta t$$

$$y_A(t + \Delta t) = y_A(t) + v_{yA}(t) \Delta t$$

$$z_A(t + \Delta t) = z_A(t) + v_{zA}(t) \Delta t$$

where $x_A(t)$, $y_A(t)$ and $z_A(t)$ are coordinates of Lagrangian point A at the current moment of time (t); $x_A(t + \Delta t)$, $y_A(t + \Delta t)$ and $z_A(t + \Delta t)$ are coordinates of the same point at the next moment of time ($t + \Delta t$); $v_{xA}(t)$, $v_{yA}(t)$ and $v_{zA}(t)$ are components of material velocity vector in the point A at the current moment of time. In case of variable velocity field the velocity of Lagrangian point A can change during the displacement and first order of accuracy scheme will not be very accurate. This problem can be resolved either by using smaller time step (Δt), or by using higher order of accuracy advection schemes.

One of the most popular in geomodeling is forth order of accuracy Runge-Kutta advection scheme.

$$x_A(t + \Delta t) = x_A(t) + v_{xA}(eff) \Delta t$$

$$y_A(t + \Delta t) = y_A(t) + v_{yA}(eff) \Delta t$$

$$z_A(t + \Delta t) = z_A(t) + v_{zA}(eff) \Delta t$$

where $v_{xA}(eff)$, $v_{yA}(eff)$ and $v_{zA}(eff)$ are components of effective material velocity vector for the point A for the period between current (t) and next ($t + \Delta t$) moments of time. Components of the effective material velocity are computed by using material velocity in four different points (A, B, C and D)

$$v_{xA}(eff) = [v_{xA}(t) + 2v_{xB}(t) + 2v_{xC}(t) + v_{xD}(t)]/6$$

$$v_{yA}(eff) = [v_{xA}(t) + 2v_{yB}(t) + 2v_{yC}(t) + v_{yD}(t)]/6$$

$$v_{zA}(eff) = [v_{zA}(t) + 2v_{zB}(t) + 2v_{zC}(t) + v_{zD}(t)]/6$$

where coordinates of points B, C and D are computed as follows

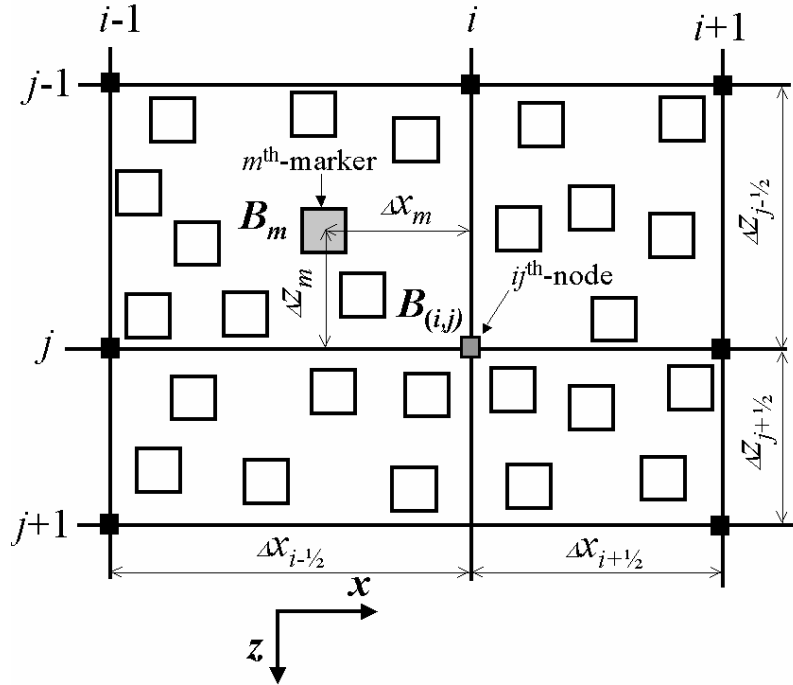
$$x_B(t) = x_A(t) + \frac{1}{2}v_{xA}(t)\Delta t, \quad y_B(t) = y_A(t) + \frac{1}{2}v_{yA}(t)\Delta t, \quad z_B(t) = z_A(t) + \frac{1}{2}v_{zA}(t)\Delta t,$$

$$x_C(t) = x_A(t) + \frac{1}{2}v_{xB}(t)\Delta t, \quad y_C(t) = y_A(t) + \frac{1}{2}v_{yB}(t)\Delta t, \quad z_C(t) = z_A(t) + \frac{1}{2}v_{zB}(t)\Delta t,$$

$$x_D(t) = x_A(t) + v_{xA}(t)\Delta t, \quad y_D(t) = y_A(t) + v_{yA}(t)\Delta t, \quad z_D(t) = z_A(t) + v_{zA}(t)\Delta t.$$

This advection scheme is extremely precise in space (fourth order of accuracy) but less precise in time (first order of accuracy) because velocity field used is for the current moment of time only.

To interpolate physical properties (e.g., density, viscosity, heat capacity) from Lagrangian markers to Eulerian nodes various interpolation scheme can be used



The following standard first order of accuracy scheme is often used to calculate an interpolated value of a parameter $B_{(i,j)}$ for ij^{th} -node using values (B_m) ascribed to all markers found in the four surrounding cells

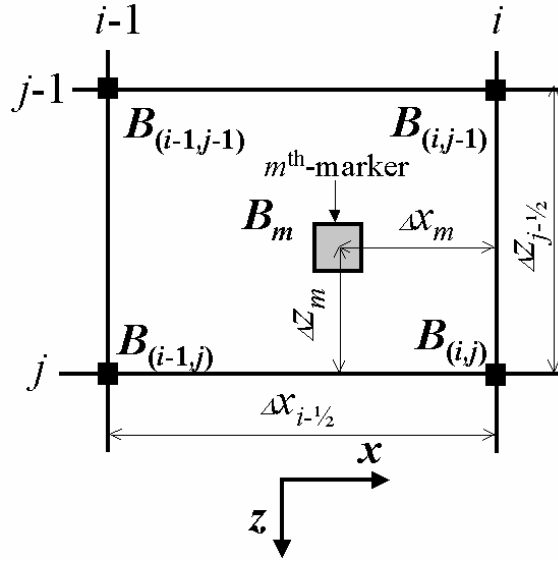
$$B_{(i,j)} = \sum_m B_m w_{m(i,j)} / \sum_m w_{m(i,j)},$$

$$w_{m(i,j)} = [1 - \Delta x_m / \Delta x_{(i-1/2)}] \times [1 - \Delta z_m / \Delta z_{(j-1/2)}],$$

where $w_{m(i,j)}$ represents a statistical weight of m^{th} -marker at the ij^{th} -node; $\Delta x_m / \Delta x_{(i-1/2)}$ and $\Delta z_m / \Delta z_{(j-1/2)}$ are normalized distances from m^{th} -marker to ij^{th} -node. The use of a higher-order accurate interpolation schemes produces undesirable numerical fluctuations in scalar, vector and tensor properties interpolated in the proximity of sharp transitions which are often present in geodynamic models.

Very often the inverse problem of interpolation of physical parameters (e.g., velocity, pressure) from Eulerian nodes to Lagrangian markers and other geometrical points has to be solved. One of the most

simple methods is to use values of a physical parameter B defined in four Eulerian nodes surrounding a given Lagrangian marker (or other given geometrical point). An effective value of the parameter B for m^{th} -marker can then be calculated with the first order interpolation scheme as follows



$$B_m = [1 - \Delta x_m / \Delta x_{(i-1/2)}] \times [1 - \Delta z_m / \Delta z_{(j-1/2)}] \times B_{(i, j)} + [\Delta x_m / \Delta x_{(i-1/2)}] \times [1 - \Delta z_m / \Delta z_{(j-1/2)}] \times B_{(i-1, j)} +$$

$$[1 - \Delta x_m / \Delta x_{(i-1/2)}] \times [\Delta z_m / \Delta z_{(j-1/2)}] \times B_{(i, j-1)} + [\Delta x_m / \Delta x_{(i-1/2)}] \times [\Delta z_m / \Delta z_{(j-1/2)}] \times B_{(i-1, j-1)},$$

where B_m denote the value of parameter B for m^{th} -marker.

LECTURE 12.

Thermomechanical code algorithm.

From a general geophysical standpoint, one should consider at least three important requirements for a numerical geodynamic modelling code:

(1.) the ability to conserve stresses under conditions involving sharply discontinuous viscosity distribution;

(2.) the ability to conserve heat and chemical fluxes in the face of sharply varying conductivity, transport coefficient and temperature gradients;

(3.) the ability to conserve scalar quantities with multiscale properties, such as temperature field, chemical species, and density in flows with a strongly advection character (e.g. subduction).

In order to achieve these goals, one can use a conservative finite-difference (FD) scheme over an irregularly-spaced staggered grid. The irregularly spaced grid is extremely useful in handling geodynamical situations with multiple-scale character, such as in a subducting slab and the wedge flow above it. This Eulerian FD method is then combined with the moving marker technique. In the Figure below a schematic flow-chart is shown for updating at each timestep the evolutionary equations:

continuity equation, Stokes equation and temperature equation. The steps are as follows:

(1) Solving continuity and Stokes equations in 2-D by directly inverting the global matrix.

(2) Calculating the nonlinear shear- and adiabatic heating terms $H_{s(i,j)}$ and $H_{a(i,j)}$ at the Eulerian nodes.

(3) Calculating $(D T/D t)_{(i,j)}$ values at the Eulerian nodes by an explicit scheme.

(4) Defining an optimal time step Δt for temperature equation. One can use a minimum time step value satisfying the following conditions: given absolute time step limit on the order of a minimal characteristic timescale for the modelled processes; given relative marker displacement step limit (typically 0.1-0.2 of minimal grid step) corresponding to calculated velocity field (see Step 1); given absolute nodal temperature change limit (typically 1-20 K) corresponding to calculated explicit $(D T/D t)_{(i,j)}$ values (see Step 3).

(5) Solving the nonlinear temperature equation implicitly by a direct Gaussian inversion method.

(6) Interpolating calculated nodal temperature changes (see Step 6 at Figure) from the Eulerian nodes to the markers and calculating new marker temperatures (${}^t T_m$).

(7) Using a fourth-order in space/first-order in time explicit Runge-Kutta scheme for advecting all markers throughout the mesh according to the globally calculated velocity field v (see Step 1).

(8) Calculating globally the scalar physical properties ($\eta_m, \rho_m, C_m, C_{p_m}, k_m, C$, etc.) from the markers.

(9) Interpolating temperature and other scalar properties, such as C , C_p , from the markers to Eulerian nodes. Returning to Step 1 at the next timestep.

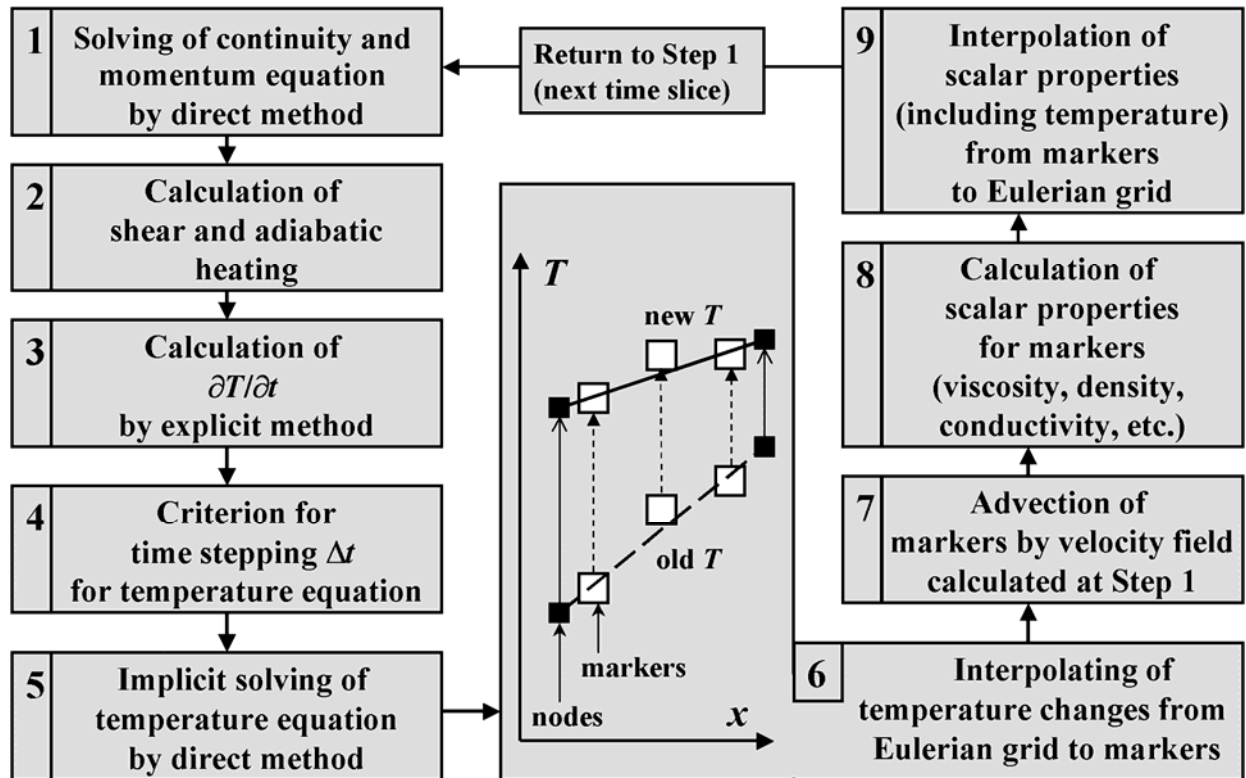


Figure. Flow chart represents structure of one of the numerical thermomechanical geodynamic code (I2VIS, Gerya & Yuen, 2003) involving finite-differences and marker-in-cell technique for solving momentum, continuity and temperature equation. Advective term in temperature equation in this code is solved by using marker-in-cell method to avoid numerical diffusion (Step 6 and 9). In case of slow advection upwind differences can be used in Step 5 and Step 6 can be omitted.